



HAL
open science

Transfer of trace organic compounds in an operational soil-aquifer treatment system assessed through an intrinsic tracer test and transport modelling

Quentin Guillemoto, Géraldine Picot-Colbeaux, D. Valdes, Nicolas Devau, Frédéric Mathurin, Marie Pettenati, Wolfram Kloppmann, Jean-Marie Mouchel

► To cite this version:

Quentin Guillemoto, Géraldine Picot-Colbeaux, D. Valdes, Nicolas Devau, Frédéric Mathurin, et al.. Transfer of trace organic compounds in an operational soil-aquifer treatment system assessed through an intrinsic tracer test and transport modelling. *Science of the Total Environment*, 2022, 836, pp.155643. 10.1016/j.scitotenv.2022.155643 . hal-03711370

HAL Id: hal-03711370

<https://brgm.hal.science/hal-03711370>

Submitted on 1 Jul 2022

HAL is a multi-disciplinary open access archive for the deposit and dissemination of scientific research documents, whether they are published or not. The documents may come from teaching and research institutions in France or abroad, or from public or private research centers.

L'archive ouverte pluridisciplinaire **HAL**, est destinée au dépôt et à la diffusion de documents scientifiques de niveau recherche, publiés ou non, émanant des établissements d'enseignement et de recherche français ou étrangers, des laboratoires publics ou privés.



Transfer of trace organic compounds in an operational soil-aquifer treatment system assessed through an intrinsic tracer test and transport modelling



Q. Guillemoto^{a,b,*}, G. Picot-Colbeaux^a, D. Valdes^b, N. Devau^a, F.A. Mathurin^a, M. Pettenati^a, W. Kloppmann^a, J.-M. Mouchel^b

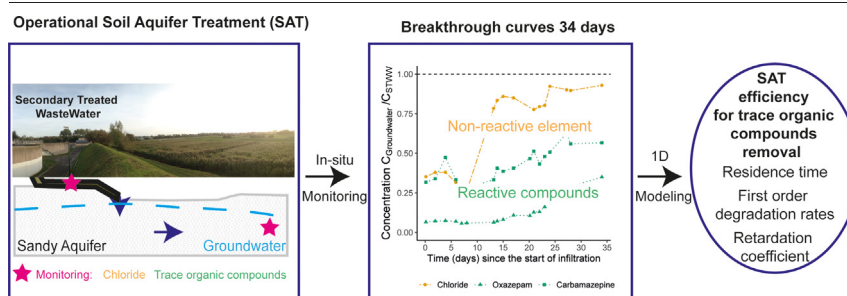
^a BRGM, French Geological Survey, 3 Av. Claude Guillemin, B.P. 6009, F-45000 Orléans, France

^b Sorbonne Université, UMR 7619 Metis, CNRS, EPHE, Paris, France

HIGHLIGHTS

- Real-life performance of an operational soil-aquifer treatment system with respect to trace organic compounds (TrOCs)
- “All-in” method using intrinsic conservative tracers through field experiment, geochemical modelling, 1D reactive transport modelling
- Errors on transport and reactive transport parameters of TrOCs were estimated through a Monte Carlo approach
- Four compounds, including carbamazepine, considered as persistent in the literature, were degraded by the investigated SAT
- Performance assessment of SAT systems based mainly on parameters that can be routinely measured under operational conditions.

GRAPHICAL ABSTRACT



ARTICLE INFO

Editor: Damià Barceló

Keywords:

Trace Organic Compounds
Soil-aquifer treatment
Reactive transport model
Sorption
Degradation

ABSTRACT

Soil Aquifer Treatment (SAT) can provide supplementary treatment of trace organic compounds (TrOCs) such as pharmaceutical and industrial compounds present in Secondary Treated Wastewater (STWW). Concern on presence of unregulated TrOCs in natural systems has raised recently as well as the interest in SAT systems for remediation. The present study quantifies, at the field scale over 35 m of lateral groundwater flow, the effectiveness of the Agon-Coutainville SAT system (Manche, Normandy, France) for TrOCs removal by sorption and biodegradation through monitoring of seven TrOCs (oxazepam, carbamazepine, benzotriazole, tolyltriazole, caffeine, paracetamol, ibuprofen) and major inorganic compounds as intrinsic tracers in STWW and groundwater during a 34-day STWW infiltration experiment during operational use of the SAT. Cationic exchanges and mixing between groundwater and STWW during the experiment were highlighted by major ions and geochemical simulations. Due to the low thickness of the unsaturated zone, a 1D analytical solution of the advection-dispersion equation (ADE) was applied on chloride data. Chloride was used as conservative intrinsic tracer to calibrate the horizontal flow and transport parameters such as the aquifer dispersion coefficient (D) and the average pore water velocity (ν) allowing estimation of the groundwater residence time. Transport and attenuation of the TrOCs were simulated assuming first-order degradation constant (μ) and linear retardation coefficient (R), calibrated to simulate the observed temporal changes in the breakthrough of TrOCs.

Abbreviations: MAR, Managed Aquifer Recharge; SAT, Soil Aquifer Treatment; TrOCs, Trace Organic Compounds; STWW, Secondary Treated Wastewater; WWTP, WasteWater Treatment Plant; ADE, Advection-Dispersion Equation.

* Corresponding author at: BRGM, French Geological Survey, 3 Av. Claude Guillemin, B.P. 6009, F-45000 Orléans, France.

E-mail address: q.guillemoto@brgm.fr (Q. Guillemoto).

<http://dx.doi.org/10.1016/j.scitotenv.2022.155643>

Received 2 March 2022; Received in revised form 28 April 2022; Accepted 28 April 2022

Available online 2 May 2022

0048-9697/© 2022 The Authors. Published by Elsevier B.V. This is an open access article under the CC BY license (<http://creativecommons.org/licenses/by/4.0/>).

Sorption was found to play a role in the transport of TrOCs, notably for oxazepam with a higher linear retardation coefficient value of 2.2, whereas no significant differences of retardation were observed for carbamazepine, tolyltriazole, benzotriazole (1.37, 1.35, 1.36 respectively). Estimated first order degradation rate constants, between 0.03d^{-1} for carbamazepine and 0.09d^{-1} for tolyltriazole, were generally high compared to the literature, possibly due to favourable redox conditions and important microbial activities within the system. This study provides evidence of the efficiency of the Agon-Coutainville SAT system for the removal of TrOCs.

1. Introduction

Managed Aquifer Recharge (MAR) is the intentional recharge of an aquifer for later recovery or environmental benefits (Dillon et al., 2020). To face an increasing water demand and maintain, enhance and secure stressed aquifers, MAR is an increasingly important water management strategy (Dillon et al., 2019; Sprenger et al., 2017).

Where recharge conditions are favourable, soil-aquifer treatment (SAT) of secondary treated wastewater (STWW) is one of the possible MAR techniques. SAT is the controlled recharge of an aquifer in order to benefit of additional pollutant removal upon infiltration through soil and the unsaturated zone (Amy and Drewes, 2007; Bekele et al., 2011; Laws et al., 2011). The use of STWW is attractive for MAR because it is a continuous source of water released daily by human activities and it is less subject to climatic change than other water sources also used in MAR systems.

However STWW contain a large range of *unregulated* Trace Organic Compounds (TrOCs) as pharmaceutical and agrochemical compounds including pesticides ... (Teijon et al., 2010; Ternes, 1998). Pharmaceutical substances are ubiquitous in sewage and, due to their variable degradability, they may only be partly removed in wastewater treatment plants (WWTP) (Biel-Maeso et al., 2018; Drewes et al., 2003). Industrial compounds include widely applied anticorrosives but are also widely present in dishwater detergents (Giger et al., 2006; Janna et al., 2011) in particular benzotriazole (BTZ) and tolyltriazole (TTZ) that may persist in the environment (Giger et al., 2006). STWW is a direct pathway for TrOCs to be introduced in the environment. Due to their toxicity, persistence and bioaccumulation, even at trace concentrations (ng/L), TrOCs can have negative effects on human health and the aquatic environment (Aemig et al., 2021; Du et al., 2014).

The fate of TrOCs namely depends on microbial transformation and/or sorption (Maeng et al., 2011 and references therein). At the field scale, the fate of TrOCs is difficult to predict because of numerous biogeochemical controlling factors, often site-specific. The reactive transport of the TrOCs will be a function of the physico-chemical properties of the molecules (i.e. Charge, hydrophobicity, functional groups) but also of the local subsurface environmental conditions (i.e. local redox conditions, microbial diversity, organic carbon and organic matter content of the sediments, mineralogy ...; Bertelkamp et al., 2014; Greskowiak et al., 2017; Patterson et al., 2011). Moreover, the hydrogeological conditions governing the groundwater flow and therefore residence times, dilution, redox conditions and temperature in the aquifer (Henzler et al., 2016), finally affect TrOCs concentrations in the groundwater. It is necessary to accurately assess the time scale of the transport of the molecules and to differentiate between dilution and effective contaminant removal (Massmann et al., 2008).

The debate concerning the level of complexity required in the models for assessing the fate of pollutants runs through the hydrological sciences, and is not absent from the MAR and SAT contexts (Kloppmann et al., 2012; Picot-Colbeaux et al., 2018). Recent field studies provide useful information for a first assessment of the removal of TrOCs with simple estimations using first-order degradation rate constants and linear adsorption coefficients (Henzler et al., 2014; Nham et al., 2015; Sanz-Prat et al., 2020) and allow comparison between study sites. However, this comparison is limited by the lack of characterisation for each field study with site-specific key factors (local environmental and flow conditions). More field experiments and quantitative evaluations of these key factors linked to TrOCs reactivity are needed to cope with the large differences in first-order degradation rate constants and sorption coefficients estimated in the field.

When studying a full size STWW infiltration system, laboratory tests are hardly able to realistically reproduce in situ conditions, especially those related to microbial activity and their variability, mainly due to difference in the considered representative elementary volumes. Quantifying the fate of TrOCs, at the scale of a SAT system using STWW is therefore a complex issue. For this purpose it is possible to apply flow and reactive transport modelling including physical, chemical and, eventually, microbiological processes (Sharma et al., 2012; Tzoraki et al., 2018). They require data with sufficient resolution in time and space to take into account substrate properties, input concentrations of compounds of interest, movement of water, mixing, individual reactions, ... At field scale, in the framework of an operational SAT application, such detailed quantitative knowledge of geochemical control factors is rarely available.

This study addresses the Agon-Coutainville site (Manche, Normandy, France) where SAT is used as a supplementary treatment step before discharge of STWW to sea in an area where shellfish is commercially grown and in an estuary important for tourism (Picot-Colbeaux et al., 2021). Its main objective is to quantify, at the field scale, the reactivity of a SAT system in the mitigation of TrOCs through sorption and biodegradation processes through a controlled STWW infiltration experiment. An in-situ monitoring program of intrinsic tracer and TrOCs in groundwater was set up from the STWW infiltration point to an observation well located 35 m downstream of the infiltration point. The TrOCs investigated in this study include pharmaceuticals, carbamazepine (CBZ), oxazepam (OXZ), paracetamol (PAR), ibuprofen (IBU), a widely used stimulant, caffeine (CAF), and industrial compounds, tolyltriazole (TTZ) and benzotriazole (BTZ). They have been detected in the STWW in a previous study (Pettenati et al., 2019) and have been selected because of their contrasting characteristics with respect to expected removal and physico-chemical properties.

The approach described in this paper consists in three steps. In a first step, temporal changes in the concentration in major ionic compounds are studied in order to describe mixing between three components (STWW, groundwater, local recharge water) and to highlight geochemical processes induced by the infiltration of STWW into the aquifer. Geochemical modelling (PHREEQC, Parkhurst and Appelo, 2013) is used to simulate the observed concentration using cation exchanges and mixing in order to identify explicitly the nature and the magnitude of the mixing and geochemical processes. In a second step, the non-reactive chloride breakthrough curve is modelled using an analytical 1D solution of the Advection Dispersion Equation (ADE) (Parker and Van Genuchten, 1984) for determining the average pore water velocity (ν) and the hydrodispersive parameters (dispersion coefficient, D). In a third step, the breakthrough curves of the TrOCs are modelled with the ADE for the calculation of first-order degradation rates (μ) and retardation coefficients (R) considering uncertainties on ν , D , and injected concentrations (STWW concentration) through a Monte-Carlo approach. These values are compared with those from other field or laboratory studies considering site-specific factors determining the reactivity of the SAT of Agon-Coutainville with respect to TrOCs.

Through close collaboration with the operator, this site provides a rare opportunity to study trace organic components at the field scale for an operating SAT system. The scale effect has been identified as a major obstacle in the evaluation of the environmental behaviour of pollutants. Upscaling, compared to experimental work (batch and column experiments) addressing decimetric or, at best, metric scale, is therefore essential to assess real-world reactive transport of TrOCs. Also, investigating a non-disturbed porous medium with already well-established microbial communities after

some years of SAT functioning, is likely to provide a more realistic estimation of transport and reactive parameters than lab-scale experiments with reconstituted soil/aquifer material. The Agon-Coutainville site allows for surveys to be conducted under controlled conditions, thus combining the advantages of field-scale surveys with the rigor of experimental work.

2. Materials and methods

2.1. Site description

The study area is located in Agon-Coutainville (Manche, Normandy, France), along the coastline of the English Channel is presented in Fig. 1. The municipality is one of the oldest seaside resorts of the Manche department and is the location of the largest shellfish aquaculture area in France. Subject to a large tidal range, the groundwater resources are prone to salinization in this coastal area, resulting in low capacity for water supply. The climate is temperate with strong seasonal variations in rainfall with the wettest month being November (108 mm/month on average) and the driest April (43 mm/month on average) over the period 2006 to 2018.

In Agon-Coutainville, a SAT scheme has been implemented as complement to activated sludge WWT for more than 20 years with a treatment capacity of 35,300 population equivalents since 2005. The STWW is infiltrated via the SAT system through a reedbed area overlying a 7–9 m thick sandy unconfined aquifer. Based on investigations carried out within a 3 year EU H2020 project, AQUANES (Pettenati et al., 2019), the secondary WWT combined with the SAT system is considered as beneficial for

seawater quality when compared to other WWT systems where the STWW is generally directly discharged in the surface water (Picot-Colbeaux et al., 2021). The direct discharge of STWW to the sea is thus disregarded in this area to guaranty sustainability and quality of shellfish production, and preserve touristic economy along the coast.

Regulatory monitoring data were acquired between 2005 and 2020 from the operator (SAUR). An average daily volume of $1471 \pm 791 \text{ m}^3$ (mean 2007–2020) of STWW is discharged every four months alternately into three reed-grown infiltrations ponds with a total surface of $35,000 \text{ m}^2$. The volume and quality of STWW are subject to important variations caused by seasonal climatic variations and touristic activities: from a mean flowrate of $895 \pm 372 \text{ m}^3/\text{d}$ and a mean BOD5 (Biological Oxygen Demand in 5 days) of $308 \pm 87 \text{ mg/L}$ in October to a mean flowrate of $2194 \pm 1076 \text{ m}^3/\text{d}$ and a mean BOD5 of $136 \pm 71 \text{ mg/L}$ in February.

The aquifer is highly transmissive ($0.0016\text{--}0.003 \text{ m}^2/\text{s}$, Pettenati et al., 2019) as it consists of coarse silt (15%), fine sand (9%) to coarse sand (51%) and becomes rich in fragments of shells with depth (Crampon et al., 2021) on top of altered clay from bedrock (schist) weathering (Dupret et al., 1987). The organic matter weight is about 4.6% (Crampon et al., 2021). Previous samples of sand at different depths allowed to quantify the fraction of organic carbon content (f_{oc}) at different depths and showed higher f_{oc} in surface samples ($f_{oc} = 1.6\%$ on 0–40 cm, $f_{oc} = 0.35\%$ on 40–80 cm) and lower f_{oc} in deeper samples ($f_{oc} = 0.26\%$ on 80–120 cm, $f_{oc} = 0.15\%$ on 120–160 cm).

Observation wells located upstream and downstream of the ponds, (Fig. 1a and b) allow monitoring of the groundwater level and groundwater

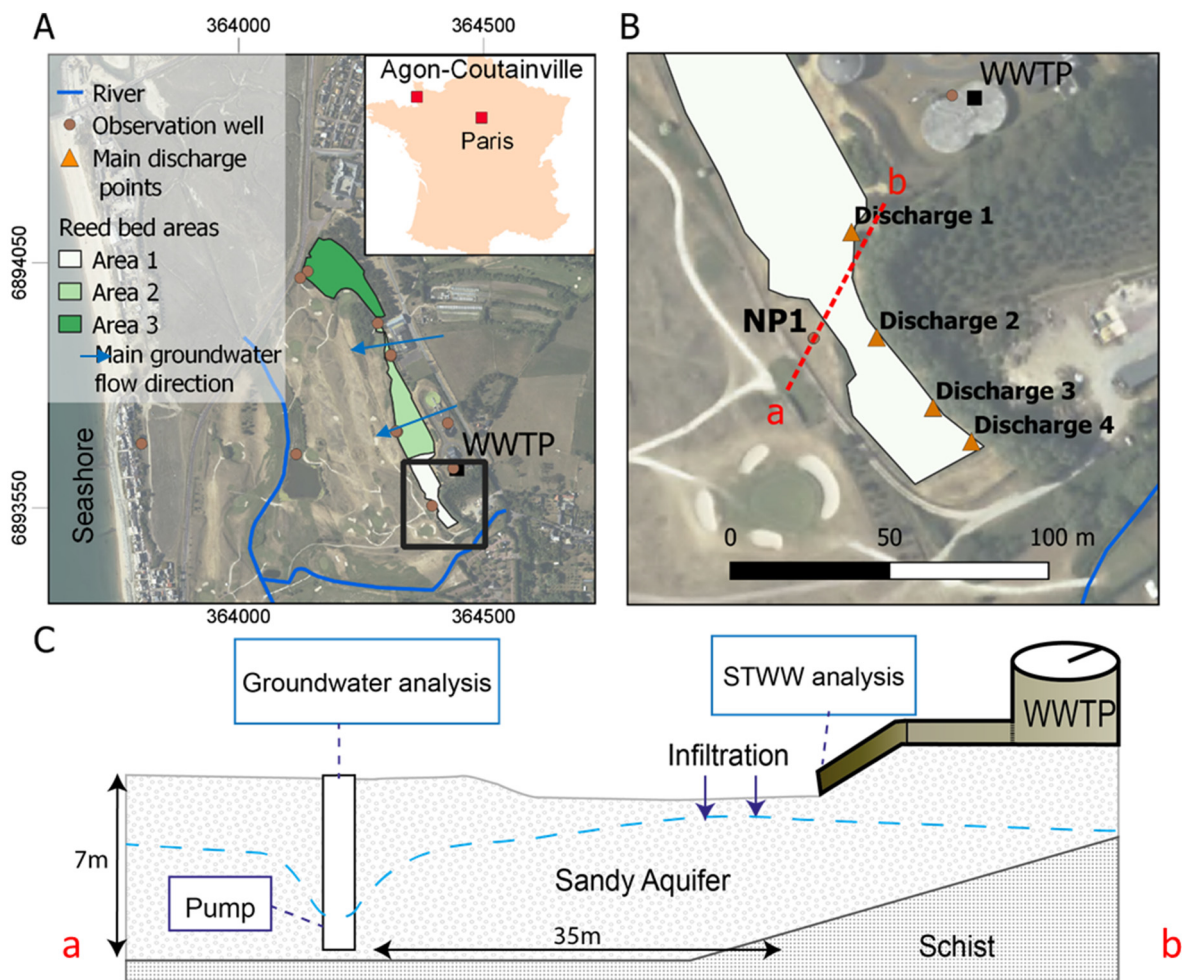


Fig. 1. Site description and conceptual model, experimental design; A) location of the Agon-Coutainville coastal operational study site with the three infiltration ponds in green and white, B) location of the infiltration pond of STWW during experimentation, C) Schematic cross section of the experimentation from the infiltration pond to the observation well NP1.

quality. Groundwater flows from the east to the west of the study site with a mean hydraulic gradient of 10^{-3} varying seasonably. Close to the pond, the groundwater flow is strongly linked to the discharged STWW flowrates. Groundwater level measurements showed that the unsaturated zone is thin: varying from a maximum of 1.5 m to zero, depending on seasonal variations and the location of the observation point with respect to the active infiltration pond.

Previous water samplings (Pettenati et al., 2019) over six field campaigns at monitoring well NP1 (Fig. 1) showed clear differences in chloride concentrations between STWW (458.5 ± 295.4 mg/L) and groundwater (123.7 ± 53.9 mg/L). TrOC concentrations are also much lower in the groundwater. As example, at NP1 observation well, mean OXZ concentrations are respectively 1882.5 ± 806.1 ng/L in STWW and 206.6 ± 126.5 ng/L in groundwater and mean CBZ concentrations 644.3 ± 367.2 ng/L in STWW and 166.8 ± 86.6 ng/L in groundwater.

2.2. Conceptual model and experimental design

The groundwater in the SAT is a mix between different endmembers: (1) regional groundwater flow, (2) local recharge by rainwater, (3) SWWT and (4) seawater intrusion.

The TrOCs concentrations in the groundwater of the SAT depend on (1) dilution of the infiltrated waters in the aquifer by the different endmembers, (2) biogeochemical mechanisms (sorption or/and degradation) occurring in soil and aquifer, and (3) microbial degradation depending on the residence time of STWW in the aquifer and thus on the groundwater flow dynamics. The latter is strongly influenced by external factors (winter recharge, individual rainfall events, tides...).

Given the multiplicity of external factors, we conducted an infiltration experiment in one of the ponds to better constrain the boundary conditions for flow and reactive transport of the TrOCs in this SAT system.

Monitoring of the resulting STWW plume in an observation well located downstream of the pond, on the main groundwater flow line provided breakthrough curves for a conservative intrinsic tracer (chloride) and the investigated TrOCs. The measurements are used to (1) quantify the admixture of STWW to the groundwater, (2) calculate the velocity/residence time of the infiltrated water and the hydrodispersive characteristics of the aquifer, and (3) estimate the reactivity of the TrOCs present in the STWW from sorption processes assessed through retardation coefficient (R) and degradation processes through first order degradation rate (μ).

The breakthrough curves are modelled using an analytical 1D solution of the Advection Dispersion Equation (ADE) (Parker and Van Genuchten, 1984) taking into account reactivity through R and μ . Simplification assumed by this solution are (1) steady-state flow in a homogeneous porous media, (2) no transversal or vertical mixing along the flow path (e.g. by local recharge) and (3) homogeneous reactivity and geochemical equilibrium along the flow path. Applied to horizontal water flow and transport through the aquifer, the use of a 1D model is justified because of the low transversal flow and the low thickness of the unsaturated zone in this homogeneous sand aquifer.

The experiment was conducted under the best possible conditions for observing strong contrasts between the ambient groundwater and the infiltrated STWW, during a period (1) with low initial TrOCs concentrations in groundwater due to a long interruption of infiltration before the experiment and (2) with low external influence, notably by local recharge (initially dry period).

2.3. Tracer test experiment

2.3.1. Experimental conditions

To measure breakthrough curves of chloride and TrOCs during STWW infiltration under conditions of operational use of the SAT, the present infiltration experiment was conducted in the southern part of the reedbed (area 1 in Fig. 1) using NP1 as observation well. The area 1 is the farthest pond from the sea, minimizing the tidal effects. To observe a significant concentration difference between STWW and groundwater, the area was not fed

by STWW for more than 8 months and the period selected corresponds to the highest pollutant concentration release in the STWW during the year. October, which is the driest month, was chosen in the aim to have the lowest interference of freshwater admixture to the STWW or directly to the groundwater (natural local recharge) during the experiment thus minimizing the effect of natural variations for the quantification of the reactivity of the system and maximizing the reactivity within the SAT. Starting from 23 October 2018 for 34 days, the STWW was released to the pond through separate outlets. The flow distribution between the four possible outlets is not controlled but depends on the hydraulic conditions in the supply pipes. During this experiment, the outlet 1 at 35 m from the observation well NP1 was mainly active (discharge point 1 in Fig. 1).

STWW and rainfall variations during the experiment are presented in the Fig. 2. The overall STWW discharged flow were measured through a Venturi channel equipped with a radar level meter and varied from 595 m³/d to 1367 m³/d, with an average of 816 m³/d. Daily variations are due to operational conditions in the WWTP and are also correlated to rain events recorded at the meteorological station located at 10 km of the study site, an increase of rainfall leading to an increase in the STWW flow rate.

The potential infiltration rate in the surface of the infiltration pond is estimated at 8 m/d. The STWW infiltrates into the aquifer at the point of discharge without any large accumulation of water on the surface. The groundwater level progressively increases from 1 m depth to the near sub-surface of the pond resulting in the water saturation of the pond bottom after two weeks. An artificial gradient from the infiltration pond to the NP1 observation well is ensured by pumping in the well (3 m³/h flow rate on average) activated five days before the beginning of the infiltration to obtain an convergent and initially permanent flow regime. Water levels (± 0.5 cm), electric conductivity ($\pm 1\%$) and temperature (± 0.1 °C) were continuously measured by a CTD-Diver probe (VanEssen) in the observation well.

2.3.2. Water sampling and analysis

For 34 days after the beginning of STWW discharge in the infiltration pond, water was sampled in the NP1 observation well and in the STWW. The NP1 water samples were collected at the pump outlet and the STWW samples at the treatment plant outlet. Samples were collected in 1 L amber glass bottles and conserved frozen until transport to the laboratory. Groundwater samples for chlorides, TrOCs and nitrates (NO₃) analysis were collected every 1–2 days during the whole experiment for a total of 17 samples in 34 days of experiment. STWW samples for chlorides, TrOCs and NO₃ were collected every day in the first week then once every week. In addition, six samples were collected once a week for major ions analysis, DOC in STWW and groundwater. For each sample, on-site measurements of pH (± 0.05), Eh (± 20 mV), temperature (± 0.1 °C), dissolved oxygen ($\pm 5\%$) were performed (WTW, Multi 3410, Germany).

Major cations (Na, Ca, Mg, K) were measured with ICP-MS, COD with sodium persulfate oxidation and major anions (Cl, NO₃, SO₄) with ion

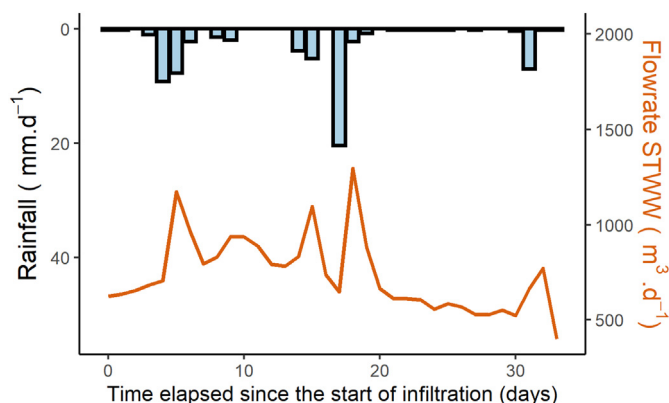


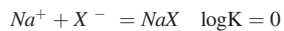
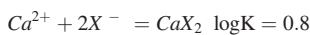
Fig. 2. Variations of rainfall (A) and STWW (B) flowrates during the experiment. Infiltration started the 23/10/2018.

chromatography. The samples were 0.45 μm filtered in-situ. For TrOCs, samples were filtered in the laboratory before analysis (GFF, 0.7 μm). Wastewater samples were diluted by a factor of 10 with demineralised Milli-Q® ultrapure water to decrease matrix effects on the chromatographic analysis. The analytical method employed for the 7 TrOCs (OXZ, CBZ, BTZ, TTZ, CAF, PAR, IBU) is online SPE extraction with Oasis HLB SPE online cartridges (Waters, France) and analysis by liquid chromatography coupled to a triple quadrupole mass spectrometer with positive and negative electrospray ionization (UPLC/MS-MS, Waters Quattro Premier XE system, Guyancourt, France) (Togola et al., 2014). Quantification of TrOCs in the environmental samples is done by internal standard calibration with a relative standard deviation of the quantification estimated around 20%. The internal standard is added to the sample before extraction for quantification. Limits of quantification (LOQ) were determined using nanopure water spiked with the target compounds with five different concentrations. The LOQ are 50 ng/L for all TrOCs except IBU, which has a LOQ of 100 ng/L.

2.4. Mixing calculations

Multi-parameter geochemical data obtained during the 34-day experiment are interpreted using the PHREEQC software and database (Parkhurst and Appelo, 2013) to estimate mixing, geochemical equilibria and water-soil interactions. Considering the chemical properties of groundwater and aquifer, sole cation exchanges reactions have been taken into account to simulate the fate of major cationic compounds.

Gaines-Thomas convention (Parkhurst and Appelo, 2013) is considered for the cation exchanges computation. The equilibrium constants for the Gaines-Thomas model as listed in Appelo and Postma (2005) are included in the PHREEQC database. Only exchange between Ca^{2+} and Na^+ predominant in initial groundwater and STWW respectively is considered here as:



X^- are the exchanges sites. The capacity of the surface to exchange cations is determined by the cation exchange capacity (CEC) in meq/L equivalent to a meq/kg of soil, usually measured in the porous media. Assumptions on porosity and specific weight of the mineral phase for the conversion to meq/kg are detailed in the Supplementary material. A CEC representative of the investigated scale could not be measured, so that we estimated an optimised value of CEC through trial and error to fit the first groundwater analysis affected by the STWW plume. CEC is then recalculated iteratively for each time step of the simulation.

In the simulations, three endmembers were taken into account: STWW, baseline groundwater (the initial concentration in groundwater) and an external endmember, local recharge water. Concentrations are available in the Supplementary material 1. STWW and groundwater concentrations were taken from the field measurements. A low Cl^- concentration of 5 mg/L was assumed for local recharge water. This estimated value relies on typical rain (e.g. Négrel et al., 2007). We also assumed that this infiltrating rainwater interacted with the soil minerals, similarly to baseline groundwater.

2.5. Flow and transport modelling

2.5.1. Analytical equilibrium ADE solution

The breakthrough curves obtained for chloride, considered as conservative tracer, and for reactive TrOCs were modelled using equilibrium analytical solutions of the one-dimensional equilibrium ADE (Parker and Van Genuchten, 1984) described by the following equation:

$$R \frac{\partial C}{\partial t} = D \frac{\partial^2 C}{\partial x^2} - v \frac{\partial C}{\partial x} - \mu C \quad (1)$$

where C [ML^{-3}] is the resident concentration of the solute in the liquid phase, x [L] the distance along the flow, t the time [T], v [LT^{-1}] the average pore water velocity defined as $v = q/n_c$ where n_c is the effective porosity and q [LT^{-1}] the Darcy velocity. D [L^2T^{-1}] is the dispersion coefficient defined as $D = \nu \alpha_L$ where α_L [L] is the longitudinal dispersivity, μ [T^{-1}] is the first-order degradation constant of the solute, and R [–] is the retardation coefficient of the solute. R and μ describe the sorption and biodegradation processes along the flow path.

The analytical (Eq. (1)) solution for the ADE is given for initial and boundary conditions. We consider a solution with (1) a constant initial concentration in groundwater assumed as $C(x,0) = C_i$, (2) a third-type inlet boundary condition with a unique pulse-type input concentration $vC(0,t) - \frac{\partial C(0,t)}{\partial x} = vC_0(t)$ with a constant infiltrated STWW concentration C_0 , (3) a lower semi-infinite boundary condition.

2.5.2. Model calibration and uncertainties

Parameters were estimated in three steps. First, an initial statistical distribution for the physical parameters (θ_p), i.e. the pore-water velocity, v , the dispersion coefficient, D , and the input concentration, C_0 , was obtained from the analysis of the conservative tracer (Cl^-) at the outlet of the WWTP and in the SAT system. Then, reactive chemical parameters (θ_c), i.e. the retardation coefficient, R , and degradation coefficient, μ , were estimated by fitting the ADE on TrOC breakthrough curves using the initial θ_p values. In a final step, the quality of the fits was optimised by adjusting iteratively both the θ_p and θ_c . The initial distribution of the transport parameters (pore-water velocity, v , and dispersion coefficient, D) was estimated by trial and error modelling of the breakthrough curve of the conservative tracer (chloride) with the ADE. The parameters v and D were adjusted to encompass the likely positions of the front given the series of observations. Following Refsgaard and Henriksen (2004), we acknowledge that the true behaviour of an open system cannot be computed due to uncertainties (on data, on unaccounted forcings) and lack of knowledge (on the real hydrodynamic behaviour). In this line, a manual calibration procedure was applied in order to stay consistent with all observations and uncertainties an automatic fit of the model would not be able to account for. Ranges of acceptable values of D and v were established using this manual procedure. The range of observed concentrations at the WWTP outlet provide an estimate for C_0 .

The parameters describing the reactive transport of TrOCs (θ_c) were estimated with the nonlinear parametric estimation package CXTFIT (Toride et al., 1995) by fitting analytical solutions to observed TrOCs data, for given sets of parameters θ_p . The CXTFIT/Excel module developed by Tang et al. (2010) was used for its great flexibility. It uses the Excel Solver to obtain a best estimate of parameter values that minimizes the sum of square of errors between observations and simulations. The quality of the fit can be described by the coefficient of determination ($r^2 = 1 - \text{SSR}/\text{SST}$, where SSR is the sum of squares of the residues and SST the sum of squares of observations).

Uncertainties on initial θ_p values were propagated by a Monte Carlo procedure. 1000 sets of plausible values of D , v and C_0 (for every TrOC) were generated. The v and D values were randomly chosen in uniform distributions covering the range of previously estimated acceptable values obtained by simulation of the chloride breakthrough curve. For C_0 , a uniform distribution covering the range of the STWW concentrations measurements during the experiment was used. Applying CXTFIT to all chosen θ_p values provides a range of values of θ_c , each of them being optimal with regards to the chosen parameters θ_p values.

The application of CXTFIT combined with the Monte Carlo procedure will also show that the quality of the fit, as measured by the r^2 values, may strongly depend on the θ_p , which means that some parameter sets appear better than others in view of TrOCs measurements.

As shown e.g. by Huet et al. (2004), in the case of independent Gaussian errors with identical variances, the least square estimator is also the maximum likelihood estimator. The underlying model can be written as follow:

$$y_i = f(t_i, \theta_p, \theta_c^*(t_i, x_i, \theta_p)) + \sigma \cdot \epsilon_i \quad (2)$$

where ϵ_i is a set of independent Gaussian random variables $N(0, 1)$ with σ their variance, and where the function f provides the values simulated by the ADE at times t_i with parameters θ_p , and with the optimal set of parameters θ_p^* obtained after applying the CXTFIT procedure with a set of x_i values with parameters θ_p . It can be rewritten as

$$y_i = g(t_i, x_i, \theta_p) + \sigma \cdot \epsilon_i \quad (3)$$

where g is the application of the ADE model using the optimised θ_p^* values. The likelihood function is

$$p(y_i; \theta_p, \sigma, x_i, t_i) = \frac{1}{(2\pi\sigma^2)^{n/2}} \exp\left(-\frac{1}{2\sigma^2} \sum_i (y_i - g(t_i, x_i, \theta_p))^2\right) \quad (4)$$

The final optimised distribution of θ_p was obtained within a Bayesian framework. The likelihood function can be seen as proportional to $p(\theta_p; t_i, x_i, \sigma)$ to provide a final distribution of parameters θ_p (the initial distributions were set as uniform as stated above). This posterior probability distribution was used as weights applied to the 1000 set of values of θ_p , to finally compute the empirical mean and variance of θ_p^* ($\bar{\theta}_p, \sigma_{\theta_p}$) since θ_p^* are functions of the θ_p .

2.5.3. Degradations and sorption parameters

First-order degradation constant (μ) are discussed in the following using the degradation half-life ($t_{1/2}$) defined as the time it takes for the concentration to drop to half of its initial value calculated as:

$$t_{1/2} = \frac{\ln 2}{\mu} \quad (5)$$

The retardation coefficient R in the ADE equation represents the effect of sorption on transport and indicates relative mobility of a particular solute defined by:

$$R = 1 + \frac{\rho_d K_d}{n} \quad (6)$$

where K_d [$L^3 M^{-1}$] is the soil-water partition coefficient, n [-] is the porosity and ρ_d [ML^{-3}] is the soil bulk density.

Retardation coefficient is further discussed considering site-specific key factors (i.e. organic matter). For organic compounds, when sorption is mainly linked to organic carbon in soils or sediments (Karickhoff et al., 1979), it is convenient to define:

$$K_d = f_{oc} \cdot K_{oc} \quad (7)$$

where f_{oc} [-] is the fraction of organic carbon, and K_{oc} [$L^3 M^{-1}$] is the soil-water partition coefficient normalised to organic carbon.

To compare the retardation between different studies, R or K_d are expressed as $\log K_{oc}$, calculated from the f_{oc} or soil bulk density and porosity of the material associated.

3. Results and discussion

The TrOCs analyses show that the concentrations of IBU and PAR fall below the quantification limit whereas those of BTZ, TTZ, OXZ, CBZ, CAF are above the quantification limit so that only the latter are presented and discussed. The Fig. 3 presents for each TrOCs and for chloride, the STWW and the groundwater concentrations for different periods: GDW_i: initial period within the first 5 days; GDW_{end}: final period in the last 10 days; and GDW_{int}: the intermediate period between the two.

Mean concentrations found in STWW are 555.8 ± 58 mg/L for Cl^- , 1875 ± 401 ng/L for BTZ, 2278 ± 607 ng/L for TTZ, 2043 ± 106 ng/L for OXZ, 750 ± 158 ng/L for CBZ and 138 ± 219 ng/L for CAF. The STWW concentrations vary during the experiment for BTZ, TTZ, CBZ, and CAF whereas they are rather constant for Cl^- and OXZ. STWW concentrations are significantly higher than those measured in the baseline groundwater GDW_i (3 times higher for Cl^- and CBZ and 6 to 14 times higher for BTZ, TTZ and OXZ). Cl^- and TrOCs concentrations increase in GDW_{int} during the experiment reaching a maximum in the GDW_{end}: from 206 mg/L to 505 mg/L for Cl^- , from less than 300 ng/L to more than 600 ng/L for BTZ, TTZ and OXA, and from 283 ng/L to 438 ng/L for CBZ. For CAF, the same tendency is not so clearly observed due to the greater variability of the measured concentrations.

The maximal concentration measured in GDW_{end} is almost equal to the concentration in STWW for Cl^- , whereas it is much lower for all the TrOCs indicating attenuation due to reactive processes compared to non-reactive Cl^- .

3.1. Identifications of mixing endmembers from major ion analysis

The application of the ADE solution based on the assumption that Cl^- concentrations are conservative requires prior identification of the water sources contributing to groundwater at the observation point and verification that breakthrough curve interpretations are not biased by the influence of saline intrusion and/or individual rainfall events that may impact the estimation of the average pore water velocity and dispersivity.

The evolution of the major ions concentrations in the groundwater and STWW during the 34-day experiment is shown on the Piper diagram (Fig. 4). Overall, the groundwater progressively approaches the STWW composition in the end of the experiment. More precisely, a displacement of the groundwater chemical composition (O1, O2, O3 and O4) is observed between two well identified endmembers: initial groundwater (at $t = 0d$) and STWW. The initial groundwater is a predominantly calcium bicarbonate water (higher Ca^{2+} concentrations) while STWW is a sodium chloride water (higher Cl^- and Na^+ concentration). Compared to the groundwater composition at $t = 6d$ which is similar to initial groundwater, the

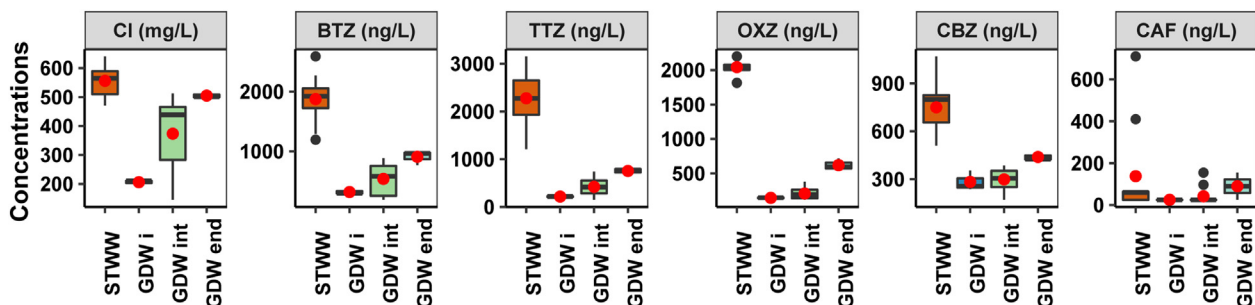


Fig. 3. Boxplot of the conservative chlorides (Cl^-) and TrOCs analysed above QL during the experiment in GDW (Groundwater) or STWW (Secondary Treated WasteWater). TrOCs are benzotriazole BTZ, tolytriazole TTZ, oxazepam OXZ, carbamazepine CBZ and caffeine CAF. GDW_i is the initial concentration in groundwater ($0d < t < 5d$); GDW_{end} the final concentration in groundwater ($25d < t < 34d$) and GDW_{int} the concentration in groundwater between initial and final concentrations ($5d < t < 25d$). The red dot is the mean values and black dots are extreme concentrations exceeding the 3rd quartile by 1.5 interquartile.

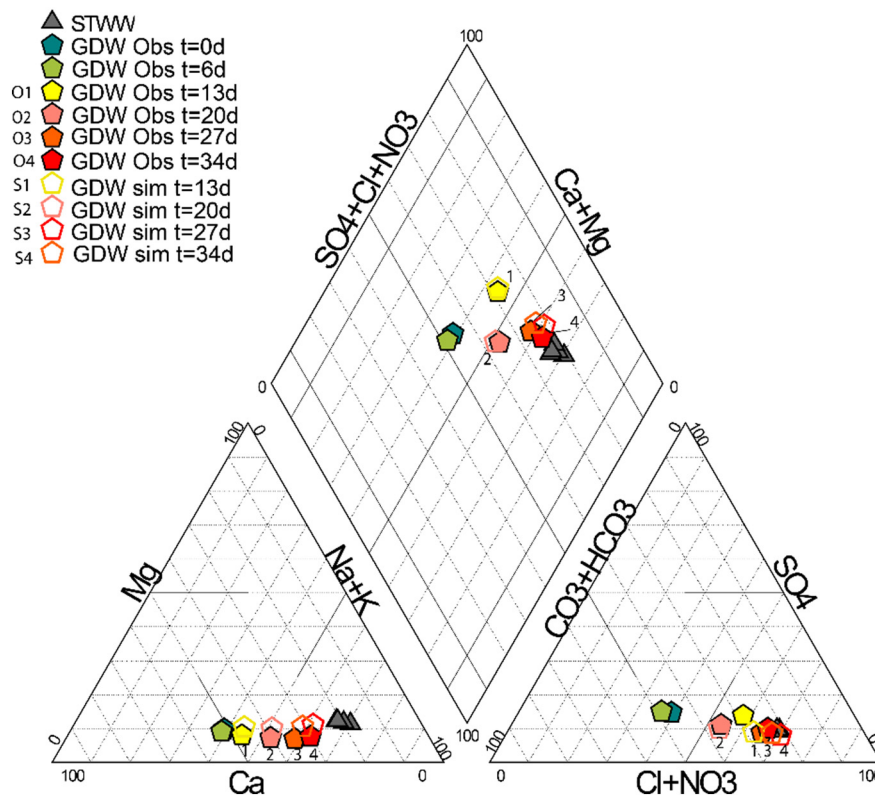


Fig. 4. Piper diagram of the major ion analysis in groundwater (GDW) and secondary wastewater (STWW) during the 34-day experiment (observations O1-O4). PHREEQC simulations (GDW sim) from $t = 13$ days to $t = 34$ days (S1-S4) mixing GDW and STWW with different proportions include ion exchange processes. The $t = 20$ day (O2) measurement point have been simulated (S2) adding mixing with an additional endmember “local recharge water”.

groundwater at $t = 13$ d, O1, is the first groundwater sample indicating a mixing with the STWW and thus the arrival of the STWW plume through the soil and aquifer.

Cations exchanges between Na^+ and Ca^+ are strongly suggested by the observations that deviate from the theoretical mixing line especially O1, O3 and O4 noticeable on cations and anions plots of the piper diagram. The disequilibrium induced by the STWW infiltration obviously causes a release of Ca^+ replaced by Na^+ on the exchanges sites in soil and aquifer.

PHREEQC simulations are used to estimate the contribution of each endmember and to reproduce the measurements considering cationic exchanges reactions. They are set up as follows: i) 3 endmembers are considered: initial baseline groundwater, STWW and local recharge water (cf. 2.4), ii) Cationic exchanges reactions are considered in all the simulations. The iteratively optimised global CEC value of soil and aquifer material (see above) is estimated as 80 meq/kg which is higher than the CEC of pure quartz of 10 meq/kg (Appelo and Postma, 2005) yet much lower than CEC of organic matter of 1500–4000 meq/kg (Appelo and Postma, 2005). This CEC value of 80 meq/kg, if we consider that all the reactivity stems from organic matter (1500–4000 meq/kg), would be equivalent to 5.3–1.7% of organic matter in the soil and aquifer which is similar to values obtained for the sands of the study site (4.6% Crampon et al., 2021). In the following, the observations (measurements) are referred to as O1 to O4 and the corresponding simulations as S1 to S4 (Fig. 4).

At $t = 13$ d, the simulation of O1 (S1 on Fig. 4) results in initial groundwater. With more than 50% STWW contribution at day 13, this simulation provides a first estimation of the mean residence time of STWW in the aquifer at less than 13 days (from the discharge point to NP1 at 35 m).

At $t = 20$ d, the chloride concentration decreases but is not accompanied by a decrease of Na or Ca concentrations (O2 and S2 on Fig. 4). Simulation of the O2 chemical composition not only indicates a 80% STWW mixing with 20% initial groundwater but also with a third endmember (35%).

The third component is probably explained by the rainfall event at $t = 17$ d (local recharge water) inducing a dilution of Cl^- concentrations.

At $t = 27$ d (O3 and S3) and $t = 34$ d (O4 and S4), the groundwater chemical compositions indicate that the STWW infiltrated water equilibrates with the aquifer chemical material and cations exchanges slightly affect the Na/Ca ratio. The simulations S3 and S4 of observations O3 and O4 result in a mixing proportion of 95% and 100% of STWW with no contribution of additional endmember indicating a total replacement of groundwater by infiltrated STWW flow at 34 days.

Except from $t = 17$ d to $t = 20$ d, when the local recharge water endmember contributes, the groundwater may be represented by a mix between only two endmembers, initial groundwater and STWW with no contribution of brackish water in the study area during the experiment. The use of the 1D ADE is thus justified to simulate the breakthrough curves between an initial state with concentrations C_i in the initial groundwater and a unique, pulse-type STWW input with concentrations C_0 .

3.2. Flow and conservative transport

3.2.1. Breakthrough curves of chlorides

The breakthrough curve of chlorides and STWW chloride concentrations are presented in the Fig. 5.

STWW Cl^- concentrations vary slightly during the experiment with a decrease from a mean concentration of 588 ± 32 mg/L over the first 6 days of the experiment to 481 ± 14 mg/L from $t = 6$ d to 34d of the experiment.

Groundwater concentration of Cl^- , shows a sharp increase in concentration between $t = 8$ d and $t = 13$ d from an initial low concentration (206 ± 8.7 mg/L, $t = 0$ d to $t = 3$ d) to a plateau concentration similar to STWW concentrations at $t = 15$ d. That confirms that STWW has totally replaced baseline groundwater in NP1 at the end of the experiment.

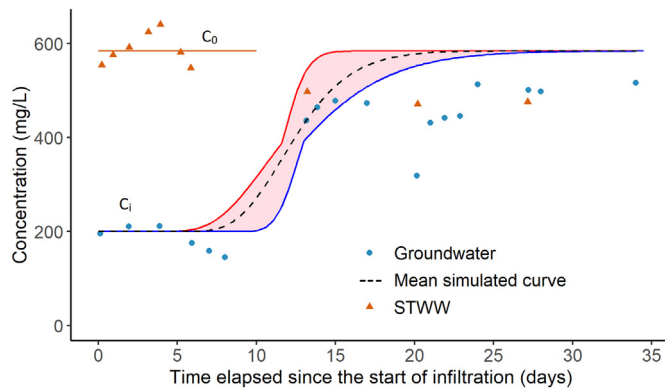


Fig. 5. Chloride measurements in STWW and breakthrough curve of chloride in groundwater at the observation well NP1. The mean curve is modelled with the 1D ADE equation using C_0 (orange horizontal line) as input STWW concentration. C_i are the initial concentration in the ADE equation. The range of non-reactive transport parameters D and ν encompass the most probable curves and simulated curves are positioned between blue and red line. The mean parameters provide the mean simulated curve.

Some external events cause minor short-term variations groundwater Cl^- concentrations during the experiment. Two rainfall events occur at $t = 4\text{d}$ and $t = 5\text{d}$ (9 mm and 8 mm) and induce a decrease in chlorides from 211 mg/L at $t = 4\text{d}$ to 145 mg/L at $t = 8\text{d}$. A more important rainy episode at $t = 17\text{d}$ (20 mm) explains the decrease of chlorides from 472 mg/L to 318 mg/L.

3.2.2. Advection-dispersion parameters

The ADE solution requires the initial Cl^- concentration of the groundwater (C_i) and the STWW (C_0). We use mean values for $t = 0\text{--}5\text{d}$, $C_i = 206\text{ mg/L}$ and $C_0 = 588\text{ mg/L}$ (Fig. 5).

By an iterative approach, ranges of values of the advection-dispersion parameters ν and D are estimated (Table 1) so that multiple possible breakthrough curves envelop the arrival of the front between $t = 8\text{d}$ and $t = 15\text{d}$ (red zone in Fig. 5). With an average pore velocity ν of 2.85 m/d (2.7 to 3 m/d) and a dispersion coefficient D of 2.75 m^2/d (0.5 to 5 m^2/d) we obtain the mean breakthrough curve shown as dashed line in Fig. 5. The dispersivity α_L is deduced from ν and D with a mean value 0.96 m (0.17 to 1.85 m) in line with previously published relationships between α_L and the investigated scale of measurements for unconsolidated sediments (Schulze-Makuch, 2005). This low value of dispersivity indicates a predominantly advective flow through this SAT system. The mean residence time of STWW is then estimated at 12.3 days (11.7 to 13.0 days).

The use of ADE solutions allows a first estimation of ν , D and α_L . Nevertheless, differences between simulated breakthrough curves and measurements remain during the plateau phase. In situ studies are complex because the external factors like rainfall or operating conditions may not be fully controlled. Rainfall dilutes wastewater and decreases concentrations and may directly influence concentrations in groundwater. These factors (dilution, C_0 variations) are not modelled by the ADE, which induces uncertainties on the estimation of ν , D . We take into account this uncertainty of the convection-dispersion parameters by defining an initially

Table 1
Flow and non-reactive transport parameters estimated with the 1D ADE resolution from the chloride breakthrough curve.

Transport parameters	Range of values		
	Lower values	Mean values	Upper values
ν average pore velocity (m/d)	2.70	2.85	3.00
D dispersion coefficient (m^2/d)	0.50	2.75	5.00
α_L longitudinal dispersivity (m)	0.17	0.96	1.85

large range of ν and D (Table 1), used in the following to estimate R and μ of reactive TrOCs. The associated errors are assessed through a Monte-Carlo approach.

3.3. Reactive transport of trace organic compounds

3.3.1. Breakthrough curves of trace organic compounds

The breakthrough curves of the TrOCs (Fig. 6) show the evolution of the STWW and groundwater concentrations during the 34-day experiment and are used for the estimation of transport and reactive parameters R and μ by applying the ADE solution for BTZ, TTZ, OXZ and CBZ. Concerning CAF, the measured concentration varies strongly in both STWW and groundwater, this high variation of CAF in STWW is often observed (Li et al., 2018), so that CAF will not be further interpreted.

In STWW, variations of TrOCs concentration are significant during the experiment. During the first week of the experiment ($t = 0\text{d}$ to $t = 6\text{d}$), mean concentrations in STWW are $1968 \pm 277\text{ ng/L}$ for BTZ, $2565 \pm 449\text{ ng/L}$ for TTZ, $2064 \pm 88\text{ ng/L}$ for OXZ and $821 \pm 121\text{ ng/L}$ for CBZ. A decreasing trend in STWW concentrations is observed reaching minimal concentrations of 510 ng/L for CBZ (at $t = 13\text{d}$), 1210 ng/L for TTZ (at $t = 27\text{d}$) and 1195 ng/L for BTZ (at $t = 20\text{d}$). Only the OXZ concentrations remain constant throughout the experiment with small variations. In groundwater, the global evolution of the TrOCs shows a low initial concentration and an increase to a maximum at the end of the experiment depending on the compounds. The initial groundwater concentrations are: 134 ng/L for OXZ, 238 ng/L for CBZ, 198 ng/L for TTZ and 370 ng/L for BTZ. TrOCs are present in the initial groundwater despite the fact that there has been no STWW discharge for more than 8 months in the pond. These concentrations suggest that the baseline groundwater is to some extent contaminated by TrOCs. The increase in concentration starts from $t = 10\text{d}$ to $t = 15\text{d}$ depending on the compounds, which is later than the Cl^- breakthrough starting at $t = 8\text{d}$, indicating a retardation for the TrOCs. Finally, the groundwater concentrations seem to reach a plateau for CBZ, TTZ, BTZ for the last three measurements of the experiment with mean concentrations of respectively $438 \pm 28\text{ ng/L}$, $755 \pm 72\text{ ng/L}$, $908 \pm 120\text{ ng/L}$, much lower than STWW concentrations measured during the first week indicating the effect of reactive processes. The increasing concentration of OXZ had not yet reached a plateau with a concentration of 715 ng/L at $t = 34\text{d}$.

The rain events during the experiment have an impact the TrOCs concentrations. The first rainfall event ($t = 4\text{--}5\text{d}$) seems to induce a slight decrease in concentration at the beginning of the experiment for BTZ, TTZ, CBZ and OXZ ($t = 5\text{--}8\text{d}$). The second rainfall event at $t = 17\text{d}$ results in a temporary decrease in groundwater concentrations for all TrOCs at $t = 20\text{d}$ when breakthrough has started, altering then the shape of the curve.

The STWW concentrations decrease strongly for BTZ, TTZ and CBZ during the experiment. The start of this decrease is difficult to define precisely. If we fix it around $t = 10\text{d}$, considering a residence time of 12d without taking into account retardation, a decrease in groundwater would be observed around $t = 22\text{d}$. Therefore, groundwater concentrations could be impacted by the decrease in STWW concentration: for TTZ and BTZ at the end of the experiment, for CBZ from the middle of the experiment. The minor decrease of OXZ in the STWW would arrive too late to have an impact on groundwater during the experiment.

To summarise, the TrOCs breakthrough curves observed are affected by (1) advection and dispersion, (2) sorption and degradation, but also (3) contribution of a local recharge water and (4) variation of the STWW concentrations and flowrates.

Hereafter, the ADE will be used to simulate the TrOCs breakthrough curves, in the aim to characterise the sorption and degradation processes, i.e. to define the R and μ parameters. However, the ADE do not take into account the variations induced by the in situ conditions: contribution of local recharge water and variation of the STWW concentrations (C_0). Therefore, results of ADE have to be interpreted carefully, considering the experimental data set. Through a Monte-Carlo approach we consider the uncertainties

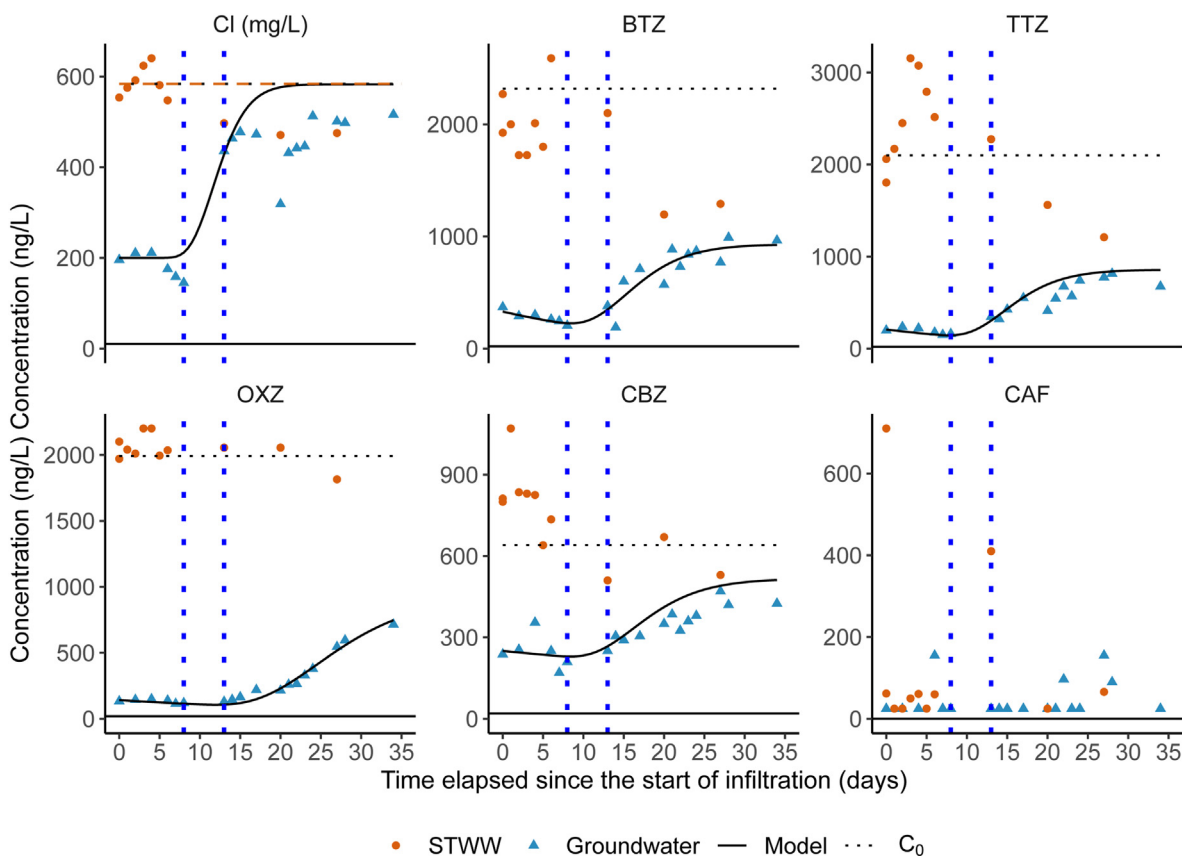


Fig. 6. Measured STWW, groundwater concentrations and simulated breakthrough curves from the 1D ADE equation. Selected parameters for the 1D ADE equation are the optimum parameters ν , D , C_0 , μ and R . The horizontal lines are the C_0 taken in the ADE from the optimum set of parameters for the TrOCs; for chloride, the C_0 is the chloride concentration in STWW the first week of the experiment. The estimated analytical error is estimated at 20%.

associated with C_0 variations, assumed, in the first instance, as constant in our ADE-based model.

3.3.2. Reactive transport parameters calculations

The reactive transport parameters were estimated with the nonlinear parametric estimation package CXTFIT (Toride et al., 1995) by fitting analytical solutions to observed TrOC data, for 1000 given sets of parameters ν and D and C_0 . The results provide optimised values of \bar{R} , $\bar{\mu}$ and their errors σ_R and σ_μ calculated from the likelihood distributions of the simulations.

The ν and D values were randomly chosen in uniform distributions covering 0.5 to 5 m²/d for D and from 2.7 to 3 m/d for ν , ranges estimated from the flow and conservative transport interpretation. The C_0 values were randomly chosen in a uniform distribution covering the range of STWW concentrations of each TrOC measured during the experiment from the maximal and minimal values: [1725, 2590] ng/L for BTZ, [1803, 3155] ng/L for TTZ, [1971, 2200] ng/L for OXZ and [510, 1070] ng/L for CBZ.

Results of the application of CXTFIT to 1000 sets of ν , D and C_0 values providing a range of values of ν and R , each of them being best fits with regards to the chosen ν , D and C_0 parameters are presented in Fig. 7. The coefficient of determination (r^2) strongly depends on the values of ν , D and C_0 which means that some parameter sets fit better than others to the TrOC measurements. The adjustment of the simulated curves to measurements (r^2) varies from 0.84 to 0.97 for OXZ, 0.80 to 0.90 for TTZ, 0.86 to 0.89 for BTZ and 0.63 to 0.87 for CBZ. The range of calculated μ at R for the 4 molecules are presented in the Table 2 to give an overview of the dispersion of the parameters. μ values vary by a factor of two for most parameter, except for CBZ with variations by a factor of eight. Values of R vary at maximum by a factor of 1.5.

The optimised average values of \bar{R} , $\bar{\mu}$ and their errors σ_R , σ_μ are calculated (Table 2) as arithmetic mean and variance values of the 1000 sets of

values of R and μ with the probability distribution of the likelihood for weights as described in 2.4.1. The final \bar{R} , $\bar{\mu}$ show a relatively high residual error for μ , especially for CBZ with a relative error of 33%. For the R , the residual relative errors are 10% to 20%.

The sensitivity of R is mainly linked (suppl. material), for all the molecules, to D and ν ; Dispersion (D) and retardation (R) act in the same sense, their augmentation decreases the slope of the concentration rise during breakthrough. Best fitting for a too low D can be achieved by an increase in R . Regarding ν , a too high value accelerates the appearance of the front, which can be compensated by an increase in R . The sensitivity of μ for the molecules CBZ, BTZ, TTZ is highly related to variations of C_0 , a lower C_0 results in higher optimised μ values to adjust the plateau concentrations measurements. For OXZ, which has not reached the concentration plateau over the experiment period, the sensitivity of μ is mainly caused by the choice of D in the simulations, which is strongly linked to R as stated before.

Simulated curves (Fig. 6) are represented using the optimised \bar{R} , $\bar{\mu}$ associated with their set of C_0 , ν and D parameters. The highest retardation coefficients are found for OXZ ($R = 2.26$). The compounds CBZ, TTZ, BTZ have lower estimated retardation ($R = 1.37, 1.35, 1.36$ respectively, Table 2). Contrarily to BTZ, TTZ, CBZ, the simulated curve of OXZ does not reach the plateau concentration, which reflects its highest retardation among the investigated TrOCs. The retardation increases the residence time of the different TrOCs and therefore the availability of the different TrOCs for biodegradation. The degradation increases the difference between the concentration plateau and the C_0 concentrations highlighting efficient degradation for BTZ, TTZ and lower degradation rates for CBZ. For OXZ, which did not reach the plateau phase, the calculated degradation rates depend on the calculated retardation value to have good adjustment between modelled curve and measurements.

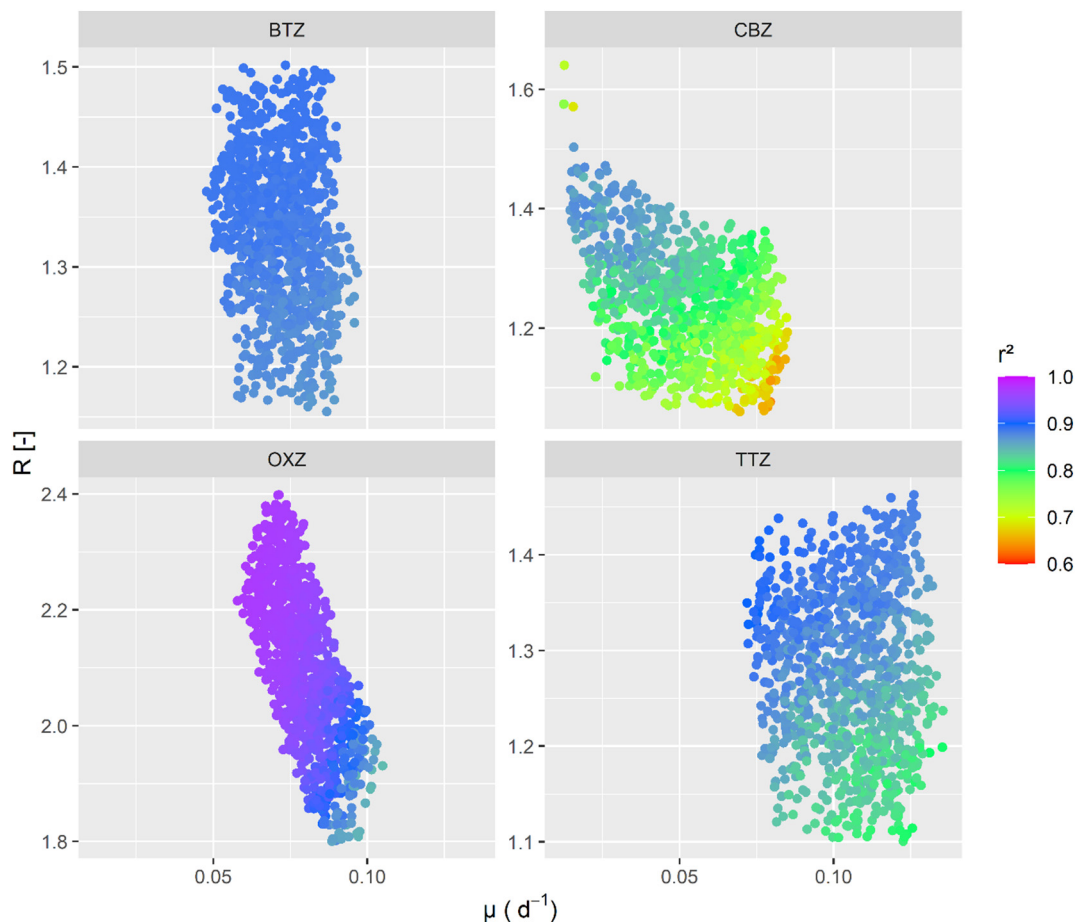


Fig. 7. Monte-Carlo simulations for oxazepam (OXZ), carbamazepine (CBZ), benzotriazole (BTZ) and tolyltriazole (TTZ). Optimal values of parameters μ and R with multiples values of D , ν and C_0 are represented by the maximal values of the coefficient of determination r^2 .

In the following, R and μ estimates, in order to compare them with literature values, physico-chemical properties will be discussed as K_{oc} and half-life ($t_{1/2}$), summarised in the Table 3.

3.3.3. Specific reactivity of the Agon-Coutainville SAT during the experiment

3.3.3.1. Retardation coefficient. The retardation coefficient R describes desorption processes along the flow. Sorption of molecules can occur through hydrophobic attraction between sediment organic matter and non-polar organic compounds (hydrophobic partitioning), or through the attraction of compounds to minerals surfaces by electrostatic forces. In order to identify the main processes affecting the TrOCs, the physico-chemical characteristics of the compounds are used as the acid dissociation constant (pKa), characterising the strength of an acid in solution, and the octanol-water coefficient K_{ow} , characterising the hydrophobicity of the molecule (Table 3).

The acid dissociation constant pKa, (Table 3) gives information on the proportion of the ionised form of the molecule taking into account the pH of the experiment (pH = 7.2–7.8). For CBZ, OXZ and TTZ, pH \ll pKa-1 shows that neutral forms are clearly the dominating species. For BTZ, the

Table 2

Main characteristics of the obtained distribution of R and μ from the 1000 simulations.

Compound	μ_{min} [d ⁻¹]	μ_{max} [d ⁻¹]	$\bar{\mu}$ [d ⁻¹]	σ_{μ} [d ⁻¹]	R_{min} []	R_{max} []	\bar{R} []	σ_R []
Oxazepam	0.05	0.10	0.07	0.01	1.80	2.40	2.26	0.07
Carbamazepine	0.01	0.08	0.03	0.01	1.06	1.64	1.37	0.06
Tolyltriazole	0.05	0.10	0.09	0.02	1.10	1.46	1.35	0.05
Benzotriazole	0.05	0.10	0.07	0.01	1.15	1.50	1.36	0.07

pKa is close to the measured pH range (i.e. pH \approx pKa-1) and therefore 20% of molecule will exist in anionic form (Table 3). Thus, for BTZ, electrostatic processes can have some impact on the sorption of the compound.

The $\log K_{ow}$ values of the TrOCs show that these compounds are low hydrophobic ($1.23 > \log K_{ow} > 2.32$) (Sabljic et al., 1995). Significant retardation for non-polar compounds with higher $\log K_{ow}$ is expected in the subsurface and it has been recognised some relationship between K_{ow} and K_{oc} (e.g. Karickhoff et al., 1979; Sabljic et al., 1995). The higher retardation coefficient estimated for OXZ in this study is consistent with the higher K_{ow} of OXZ. Some differences from the $\log K_{ow}$ variations were nevertheless expected between TTZ, CBZ and BTZ. The molecules being low hydrophobic, relations between K_{ow} and K_{oc} have limitations (Karickhoff et al., 1979) so that the use of correlations to predict neutral low hydrophobic sorption behaviour is equally limited (Kiecak et al., 2019; Schaffer et al., 2012; Yamamoto et al., 2009).

In our study, due to the low part of electrostatic processes involved for the studied TrOCs, the main sorption process we consider here is hydrophobic sorption mainly driven by the organic matter. The first meters of infiltration contain higher proportion of organic matter, the main material for the sorption of these compounds. In the study site the measured f_{oc} in surface samples was higher (1.6%, 0–40 cm) compared to deeper samples (f_{oc} = 0.15%, 120–160 cm) as observed in other SAT sites (e.g. Chefetz et al., 2008; Muntau et al., 2017). As the sorption of hydrophobic and neutral TrOCs is mainly driven by the organic carbon of the porous medium we use the K_{oc} calculated values of this experiment for comparison with experimental literature values.

The K_d calculated from the R (Eq. (6)) is normalised to the organic carbon fraction of the sediment (f_{oc} , corresponding to surface or deeper sample of the aquifer) to obtain K_{oc} values (Eq. (7)). The K_d for the different TrOCs

Table 3

Physico-chemical properties of the compounds, calculated values of the K_{oc} (*using surface sample $f_{oc} = 1.6\%$, ** using deeper sample with $f_{oc} = 0.15\%$ in the aquifer) and calculated $t_{1/2}$ values in this study, literature experimental values of $t_{1/2}$ and K_{oc} .

Compound	Physico-chemical properties			Calculated values			Literature experimental values	
	$\log K_{ow}$	pKa ^d	Ion (%) ^b	$t_{1/2}$ [d]	$\log K_{oc}$ [L/kg]	$\log K_{oc}^*$ [L/kg]	$t_{1/2}$ [d]	$\log K_{oc}$ [L/kg]
Oxazepam	2.32 ^a	10.90	0.08	10 ± 0.7	15.3 ± 4.7	2.3 ± 0.3	54 ^l , >50 ^k , >100 ^j	[2.7 ^o -2.4 ^o , 2.2 ^l]
Carbamazepine	2.25 ^a	>13.9	0.00	23 ± 7	4.6 ± 1.4	1.8 ± 0.2	No deg ^{e, f, g, h, i, 35^l}	[2.2-2.6 ^q , 1.4-1.9 ^r , 1.6 ^s]
Tolytriazole	1.89 ^c	9.92	0.75	7 ± 1.2	4.3 ± 1.3	1.8 ± 0.2	29 ^m , 31-76 ⁿ , no deg ^m , variable ⁱ	1.6 ^c -2.0 ^c , 2.4 ^p
Benzotriazole	1.23 ^c	8.37	21.21	10 ± 1.4	4.4 ± 1.4	1.8 ± 0.2	no deg ^m , 0.06 ^m , variable ⁱ , 43-83 ⁿ	1.5 ^c -1.9 ^c

^a US Environmental Protection Agency's EPISuite™ KOWWIN v.1.67.

^b Percentage of anionic form = $1 / (1 + 10^{pH-pKa}) \times 100$.

^c Hart et al. (2004).

^d PubChem database, n.d. (<https://pubchem.ncbi.nlm.nih.gov>).

^e Drewes et al. (2003).

^f Maeng et al. (2011).

^g Hellauer et al. (2018).

^h Bertelkamp et al. (2014).

ⁱ Sanz-Prat et al. (2020).

^j Patterson et al. (2010).

^k Patterson et al. (2011).

^l Löffler et al. (2005).

^m Hellauer et al. (2018).

ⁿ Liu et al. (2013).

^o Stein et al. (2008).

^p Burke et al. (2013).

^q Chefetz et al. (2008).

^r Kiecak et al. (2019).

^s Hebig et al. (2017).

^t Regnery et al. (2015).

of the experiment is calculated using the soil bulk density of 1.59 g/cm³, calculated from the quartz apparent density = 2.65 g/cm³ (Appelo and Postma, 2005) and a porosity of 0.4 ± 0.1. The $\log K_{oc}$ calculated values for OXZ, CBZ, BTZ, TTZ for different f_{oc} values (1.6% and 0.15%) are summarised in the Table 3.

To compare the K_{oc} values, the K_d or R are therefore normalised with respect to their associated f_{oc} values (or Total Organic Carbon) close to our study (Table 3). For OXZ, $\log K_{oc}$ values in the literature fall between 2.7 and 2.4 L/kg (Stein et al., 2008). For TTZ, $\log K_{oc}$ values found in the literature were in the range of 1.6–2.0 L/kg (Hart et al., 2004) to 2.4 L/kg (Burke et al., 2013) and for BTZ the range from 1.5–1.9 (Hart et al., 2004). For CBZ, $\log K_{oc}$ literature values were in the range of 1.4–2.6 L/kg (Chefetz et al., 2008; Kiecak et al., 2019).

The f_{oc} value of 0.15% representative of deeper samples in the aquifer leads to K_{oc} values that compare well with the literature, unlike the value of 1.6%. The water flow passes through the first meter of the infiltration pond were organic matter is higher to a deeper aquifer containing lower organic carbon. Knowing that, the overall sorption over the 35 m of aquifer is low compared to the sorption expected over the first meter of the water flow. A detailed monitoring near the infiltration zone could allow us to discriminate the part of sorption at the beginning of infiltration.

3.3.3.2. First order degradation rates. Losses arising from biodegradation processes are frequently explained by first order degradation. The first order degradation rates estimated here might to some extent be influenced by local recharge water dilution given the field study conditions. However, the rainfall events mentioned above are punctual, and only slightly modify the groundwater TrOC concentrations. Also, the estimated degradation rates could integrate some irreversible sorption, but further research is required to test the importance this process. The degradations rates are discussed and compared to the literature expressed as half-life ($t_{1/2}$, Eq. (5)) (Table 3).

In a review of different column experiment studies, Greskowiak et al. (2017) showed that oxic conditions enhance degradation for the majority of organic compounds. The same study showed that no general conclusions could be drawn from field studies, considering that no clear distinction could be made between oxic and anoxic rate constants in such studies.

Upon and after infiltration, the STWW transits from the oxic infiltration pond through the unsaturated zone (possibly oxic) to the saturated zone (anoxic if organic matter supply and microbial activities are sufficient). Beside these general assumptions, TrOCs biodegradation processes are very site-specific and compounds-specific (Greskowiak et al., 2017). At the beginning of the experiment, the pond had not been fed during several months inducing oxic and carbon-limited conditions. During the experiment, redox measurement showed constant oxic conditions ($E_h = 307 \pm 49$ mV) in the NP1 observation well. At the bottom of the infiltration pond, the organic carbon input of the STWW (DOC = 7.8 mg/L during the experiment) might induce anoxic conditions during the experiment.

For OXZ, some studies highlighted the persistent behaviour of this molecule (Burke et al., 2017; Patterson et al., 2010, 2011) under anaerobic and aerobic conditions (columns studies). In the context of the soil in the Agon-Coutainville study site, Crampon et al. (2021) through a batch biodegradation study found a $t_{1/2} = 3.6$ days for OXZ, mainly explained by the bacterial community present in the first meter. In our study, the half-life calculated is 10 ± 0.7 d which highlights higher degradation from other study and lower degradation than Crampon et al. (2021). The microbial communities present in the Agon-Coutainville SAT are supposed to be well adapted to the TrOCs due to more than 20 years of regular inputs from WWTP (Crampon et al., 2021) which can enhance the degradation of the TrOCs. Compared to Crampon et al. (2021) based on column-scale surface soils sample, the lower degradation estimated here can be explained by the lower microbial activity on the major part of the flow path compared to the degradation in the first meter of infiltration.

BTZ and TTZ were previously studied in SAT. Hübner et al. (2012) showed low removal during SAT (<10%) for both compounds. Hellauer et al. (2018) assumed no degradation for modelling purposes of BTZ and TTZ for conventional SAT systems, results contrasted with lower half-life time ($t_{1/2}$) for BTZ (1.5d) and TTZ (29.6d) when combining two infiltration steps with an intermediate aeration to establish more favourable oxic and carbon-limited conditions. Sanz-Prat et al. (2020) deduced from modelling a slight degradation depending on the seasons and temperatures. From laboratory experiments, Liu et al. (2011) observed very low degradation of BTZ ($t_{1/2} = 114-315$ d) and TTZ ($t_{1/2} = 14-41$ d) under different redox conditions where aerobic biodegradation showed to be the dominant natural

attenuation mechanism. Liu et al. (2013) obtained $t_{1/2} = 43\text{--}83\text{d}$ for BTZ and $t_{1/2} = 31\text{--}76\text{d}$ for TTZ depending on the redox conditions in different sediment materials with highest degradation losses under aerobic conditions. Under certain oxic/suboxic conditions, Burke et al. (2014) showed redox- and temperature-dependant degradation; higher temperatures hence enhanced microbial activity and more reducing conditions resulted in a $t_{1/2} = 7\text{d}$ for TTZ, meanwhile, no degradation was found for BTZ. Redox conditions seem to affect the degradation rates but no clear rules can be derived from the literature values. In our study, the half-life estimated for BTZ and TTZ are $9.9 \pm 1.4\text{d}$ and $7.4 \pm 1.2\text{d}$ respectively, approaching some of the half-life values of the literature. Combined oxic and anoxic conditions along the flowpath of our experiment, and long-term adaptation of the biomass might enhance the degradation of both compounds.

CBZ biodegradation is almost null in most studies from laboratory experiments (e.g.; Hellauer et al., 2019; Maeng et al., 2011; Patterson et al., 2010), and due to its presence in STWW, CBZ has been used as a STWW tracer (Cary et al., 2013; Clara et al., 2004). On field scale, no degradation is observed (Drewes et al., 2003; Muntau et al., 2017) and for modelling purposes, $t_{1/2} > 433\text{d}$ and 66d were necessary for Henzler et al. (2014) and Sanz-Prat et al. (2020) respectively to explain the observed CBZ behaviour. On soil column experiments, Regnery et al. (2015) obtained a $t_{1/2}$ of 35.2d under suboxic conditions meanwhile no ($t_{1/2} > 700\text{d}$) and very low ($t_{1/2} = 106\text{d}$) degradation under anoxic and oxic conditions were observed for CBZ. The optimised half-life estimated by this study is $23 \pm 7\text{d}$. This half-life is found lower than most literature values but approaches estimations of Regnery et al. (2015) for suboxic redox conditions. Uncertainties remain high in the estimation of $t_{1/2}$ for CBZ due to its high STWW variations relative to the low concentrations in groundwater so that even low variations due to external events (local natural recharge) would affect strongly the degradations rates estimations. Nevertheless, as observed for OXZ, in-situ conditions can enhance the biomass activity during the infiltration and the combined condition of oxic and anoxic redox conditions might increase the biodegradation of a compound as CBZ traditionally considered as persistent.

The results show an efficient degradation of BTZ and TTZ within the SAT taking into account the variability of transport parameters and STWW variations concentrations through the method used here. CBZ and OXZ showed higher degradation rates in the Agon-Coutainville SAT than other studies, mainly explained by the long-term adaptation of the SAT system to STWW and by the redox conditions through the flow; furthermore, given the uncertainty on the $t_{1/2}$ for CBZ, more research will be necessary to verify efficiency of this SAT system.

In the objective of prediction, the estimated parameters give a first idea of the reactivity of the SAT system but extrapolation to a larger scale will require further investigations since the major part of biodegradation and retardation is expected to take place over the first meters of flow. Nevertheless, these estimations provide evidence of the degradation of TrOCs that can be expected until the outflow of the groundwater (river, sea, harbour). The extrapolation of the reactive parameters estimated here to other study sites is not advised, as a huge variability of rate constants are highlighted between different studies, even for comparable approaches and investigation scales, there is an uncertainty on the degradation rates and on the influencing factors and processes involved (Greskowiak et al., 2017).

4. Conclusions

In this study, an experimental design is proposed for the quantification of the flow and transport characteristics of an aquifer and the estimation of transport and reactive parameters of TrOCs through sorption and biodegradation during their transport at field scale. Our methodology is applicable under operational conditions of real-world SAT systems.

It combines (1) monitoring of intrinsic tracers (major ions including chloride as conservative tracer) and of TrOCs during controlled STWW infiltration, (2) the use of ADE to estimate mean residence time and

dispersive parameter D , (3) best-fit algorithms and a Monte-Carlo approach to estimate the reactive parameters R and μ and their uncertainties.

Applied to the Agon-Coutainville study site, results highlight the supplementary mitigation of the residual TrOCs after secondary wastewater treatment provided by SAT, due to sorption and degradation processes. Cationic exchanges are observed from the major ions analysis, possibly also related to the organic matter content of the sands. Retardation of TrOCs is observed during the transfer through soil and aquifer. A slightly higher retardation for OXZ compared to other TrOCs is mainly explained by the $\log K_{ow}$ of the molecule through hydrophobic sorption onto the organic matter but no differences were found for CBZ, TTZ, BTZ. The compounds OXZ, TTZ, BTZ, and CBZ considered as relatively persistent in the literature, were degraded by the SAT on this site possibly due to favourable redox condition and important microbial activities within a system already in place for several years. The identified reactive parameters are averaged spatially in our study, but the strongest reactivity is expected at the beginning of the infiltration. To confirm the hypothesis of spatial variations of reactivity within the SAT, studies with a higher spatial resolution are recommended.

The strength of our method lies in the simplicity and robustness of the measurements and interpretation of hydrochemical data so that it can be adapted to other SAT field studies under the conditions of operational use. Considering the technical and financial constraints of an operating SAT, the methodology presented here can provide operators with important information on reactive transport parameters to estimate the efficiency of the SAT for the removal of TrOCs.

At a larger temporal and spatial scale, compared to our experiment, the transient effects (i.e. natural recharge, tides, STWW flow and concentration variations) can have important impacts on the purifying effect of SAT on TrOCs due to modification of residence time and water mixing proportions. Using transient modelling tools, further investigation of the Agon-Coutainville SAT is planned to determine the impact of these variations on the SAT efficiency and to accurately assess the fate of TrOCs in such natural systems.

At the laboratory scale of investigation, further investigations of the site-specific factors (i.e. in-situ redox conditions, key enzymes of the microbial community, composition of the organic matter...) coupled with the investigation of degradation pathways are needed to identify key factors triggering the degradations and sorption processes in this specific SAT system. These key factors of TrOCs are still poorly understood in such field-scale SAT systems.

CRedit authorship contribution statement

All authors contributed to the study conception and design. Material preparation, data collection and analysis were performed by Picot-Colbeaux G., Devau N. and Mathurin F.A. Data proofreading and technical support were performed by Valdes D., Pettenati M., Kloppmann W., Mouchel J-M. The first draft of the manuscript was written by Guillemoto Quentin and all authors commented on previous versions of the manuscript. All authors read and approved the final manuscript.

Declaration of competing interest

The authors declare that they have no known competing financial interests or personal relationships that could have appeared to influence the work reported in this paper.

Acknowledgments

This work has been performed in the frame of the EU Water JPI (Joint Programming Initiative "Water Challenges for a Changing World") within the research projects EviBan (evidence based assessment of NWRM for sustainable water management EviBAN - ANR-18-WTW7-0008-ERA-NET Cofund WaterWorks - 2018) and AquaNES (Demonstrating synergies in combined natural and engineered processes for water treatment system under grant agreement no. 689450). We gratefully thank Eric Dufour, Didier

Allain and Mickaël Gosselin (SAUR) for their field support and their data share as well as Yamen Ouerghi (BRGM) and the municipality of Agon-Coutainville who facilitated the implementation of the experiment.

Appendix A. Supplementary material

Supplementary material to this article can be found online at <https://doi.org/10.1016/j.scitotenv.2022.155643>.

References

- Aemig, Q., Hélias, A., Patureau, D., 2021. Impact assessment of a large panel of organic and inorganic micropollutants released by wastewater treatment plants at the scale of France. *Water Res.* 188, 116524. <https://doi.org/10.1016/j.watres.2020.116524>.
- Amy, G., Drewes, J., 2007. Soil aquifer treatment (SAT) as a natural and sustainable wastewater reclamation/reuse technology: fate of wastewater effluent organic matter (EfOM) and trace organic compounds. *Environ. Monit. Assess.* 129, 19–26. <https://doi.org/10.1007/s10661-006-9421-4>.
- Appelo, C.A.J., Postma, D., 2005. *Geochemistry, Groundwater and Pollution*. 2nd ed. CRC Press, Taylor & Francis Group, Boca Raton London New York.
- Bekele, E., Toze, S., Patterson, B., Higginson, S., 2011. Managed aquifer recharge of treated wastewater: water quality changes resulting from infiltration through the vadose zone. *Water Res.* 45, 5764–5772. <https://doi.org/10.1016/j.watres.2011.08.058>.
- Bertelkamp, C., Reungoat, J., Cornelissen, E.R., Singhal, N., Reynisson, J., Cabo, A.J., van der Hoek, J.P., Verliefde, A.R.D., 2014. Sorption and biodegradation of organic micropollutants during river bank filtration: a laboratory column study. *Water Res.* 52, 231–241. <https://doi.org/10.1016/j.watres.2013.10.068>.
- Biel-Maeso, M., Corada-Fernández, C., Lara-Martín, P.A., 2018. Monitoring the occurrence of pharmaceuticals in soils irrigated with reclaimed wastewater. *Environ. Pollut.* 235, 312–321. <https://doi.org/10.1016/j.envpol.2017.12.085>.
- Burke, V., Treumann, S., Duennbier, U., Greskowiak, J., Massmann, G., 2013. Sorption behavior of 20 wastewater originated micropollutants in groundwater — column experiments with pharmaceutical residues and industrial agents. *J. Contam. Hydrol.* 154, 29–41. <https://doi.org/10.1016/j.jconhyd.2013.08.001>.
- Burke, V., Greskowiak, J., Asmuß, T., Bremermann, R., Taute, T., Massmann, G., 2014. Temperature dependent redox zonation and attenuation of wastewater-derived organic micropollutants in the hyporheic zone. *Sci. Total Environ.* 482–483, 53–61. <https://doi.org/10.1016/j.scitotenv.2014.02.098>.
- Burke, V., Greskowiak, J., Grünbaum, N., Massmann, G., 2017. Redox and temperature dependent attenuation of twenty organic micropollutants - a systematic column study. *Water Environ. Res.* 89, 155–167. <https://doi.org/10.2175/106143016X14609975746000>.
- Cary, L., Casanova, J., Gaaloul, N., Guerrot, C., 2013. Combining boron isotopes and carbamazepine to trace sewage in sanitized groundwater: a case study in Cap Bon, Tunisia. *Appl. Geochem.* 34, 126–139. <https://doi.org/10.1016/j.apgeochem.2013.03.004>.
- Chefetz, B., Mualem, T., Ben-Ari, J., 2008. Sorption and mobility of pharmaceutical compounds in soil irrigated with reclaimed wastewater. *Chemosphere* 73, 1335–1343. <https://doi.org/10.1016/j.chemosphere.2008.06.070>.
- Clara, M., Strenn, B., Kreuzinger, N., 2004. Carbamazepine as a possible anthropogenic marker in the aquatic environment: investigations on the behaviour of carbamazepine in wastewater treatment and during groundwater infiltration. *Water Res.* 38, 947–954. <https://doi.org/10.1016/j.watres.2003.10.058>.
- Crampon, M., Soulier, C., Sidoli, P., Hellal, J., Joulian, C., Charron, M., Guillemoto, Q., Picot-Colbeaux, G., Pettenati, M., 2021. Dynamics of soil microbial communities during diazepam and oxazepam biodegradation in soil flooded by water from a WWTP. *Front. Microbiol.* 12, 742000. <https://doi.org/10.3389/fmicb.2021.742000>.
- Dillon, P., Stuyfzand, P., Grischek, T., Lfluria, M., Pyne, R.D.G., Jain, R.C., Bear, J., Schwarz, J., Wang, W., Fernandez, E., Stefan, C., Pettenati, M., van der Gun, J., Sprenger, C., Massmann, G., Scanlon, B.R., Xanke, J., Jokela, P., Zheng, Y., Rossetto, R., Shamruk, M., Pavelic, P., Murray, E., Ross, A., Bonilla Valverde, J.P., Palma Nava, A., Ansems, N., Posavec, K., Ha, K., Martin, R., Sapiano, M., 2019. Sixty years of global progress in managed aquifer recharge. *Hydrogeol. J.* 27, 1–30. <https://doi.org/10.1007/s10040-018-1841-z>.
- Dillon, P., Fern, E., Massmann, G., 2020. *Managed Aquifer Recharge for Water Resilience*. 11. Drewes, J.E., Heberer, T., Rauch, T., Reddersen, K., 2003. Fate of pharmaceuticals during ground water recharge. *Groundw. Monit. Remediat.* 23, 64–72. <https://doi.org/10.1111/j.1745-6592.2003.tb00684.x>.
- Du, B., Price, A.E., Scott, W.C., Kristofco, L.A., Ramirez, A.J., Chambliss, C.K., Yelderman, J.C., Brooks, B.W., 2014. Comparison of contaminants of emerging concern removal, discharge, and water quality hazards among centralized and on-site wastewater treatment system effluents receiving common wastewater influent. *Sci. Total Environ.* 466–467, 976–984. <https://doi.org/10.1016/j.scitotenv.2013.07.126>.
- Dupret, L., Poncet, J., Lautribou, J.P., Hommeril, P., 1987. Notice explicative de la feuille coutances à 1/50 000.
- Giger, W., Schaffner, C., Kohler, H.-P.E., 2006. Benzotriazole and tolyltriazole as aquatic contaminants. 1. Input and occurrence in rivers and lakes. *Environ. Sci. Technol.* 40, 7186–7192. <https://doi.org/10.1021/es061565j>.
- Greskowiak, J., Hamann, E., Burke, V., Massmann, G., 2017. The uncertainty of biodegradation rate constants of emerging organic compounds in soil and groundwater – a compilation of literature values for 82 substances. *Water Res.* 126, 122–133. <https://doi.org/10.1016/j.watres.2017.09.017>.
- Hart, D.S., Davis, L.C., Erickson, L.E., Callender, T.M., 2004. Sorption and partitioning parameters of benzotriazole compounds. *Microchem. J.* 77, 9–17. <https://doi.org/10.1016/j.microc.2003.08.005>.
- Hebig, K.H., Groza, L.G., Sabourin, M.J., Scheytt, T.J., Ptacek, C.J., 2017. Transport behavior of the pharmaceutical compounds carbamazepine, sulfamethoxazole, gemfibrozil, ibuprofen, and naproxen, and the lifestyle drug caffeine, in saturated laboratory columns. *Sci. Total Environ.* 590–591, 708–719. <https://doi.org/10.1016/j.scitotenv.2017.03.031>.
- Hellauer, K., Karakurt, S., Sperlich, A., Burke, V., Massmann, G., Hübner, U., Drewes, J.E., 2018. Establishing sequential managed aquifer recharge technology (SMART) for enhanced removal of trace organic chemicals: experiences from field studies in Berlin, Germany. *J. Hydrol.* 563, 1161–1168. <https://doi.org/10.1016/j.jhydrol.2017.09.044>.
- Hellauer, K., Martínez Mayerlen, S., Drewes, J.E., Hübner, U., 2019. Biotransformation of trace organic chemicals in the presence of highly refractory dissolved organic carbon. *Chemosphere* 215, 33–39. <https://doi.org/10.1016/j.chemosphere.2018.09.166>.
- Henzler, A.F., Greskowiak, J., Massmann, G., 2014. Modeling the fate of organic micropollutants during river bank filtration (Berlin, Germany). *J. Contam. Hydrol.* 156, 78–92. <https://doi.org/10.1016/j.jconhyd.2013.10.005>.
- Henzler, A.F., Greskowiak, J., Massmann, G., 2016. Seasonality of temperatures and redox zonation during bank filtration – a modeling approach. *J. Hydrol.* 535, 282–292. <https://doi.org/10.1016/j.jhydrol.2016.01.044> In press.
- Hübner, U., Miehle, U., Jekel, M., 2012. Optimized removal of dissolved organic carbon and trace organic contaminants during combined ozonation and artificial groundwater recharge. *Water Res.* 46, 6059–6068. <https://doi.org/10.1016/j.watres.2012.09.001>.
- Huet, S., Bouvier, A., Poursat, M.-A., Jolivet, E., 2004. *Statistical Tools for Nonlinear Regression: A Practical Guide With S-PLUS And R Examples*. 2nd ed. Springer Series in Statistics. Springer, New York.
- Janna, H., Scrimshaw, M.D., Williams, R.J., Churchley, J., Sumpter, J.P., 2011. From dishwasher to tap? Xenobiotic substances benzotriazole and tolyltriazole in the environment. *Environ. Sci. Technol.* 45, 3858–3864. <https://doi.org/10.1021/es103267g>.
- Karickhoff, S., Brown, D., Scott, T., 1979. Sorption of hydrophobic pollutants on natural sediments. *Water Res.* 13, 241–248. [https://doi.org/10.1016/0043-1354\(79\)90201-X](https://doi.org/10.1016/0043-1354(79)90201-X).
- Kiecak, A., Sassiné, L., Boy-Roura, M., Elsner, M., Mas-Pla, J., Le Gal La Salle, C., Stumpp, C., 2019. Sorption properties and behaviour at laboratory scale of selected pharmaceuticals using batch experiments. *J. Contam. Hydrol.* 225, 103500. <https://doi.org/10.1016/j.jconhyd.2019.103500>.
- Kloppmann, W., Aharoni, A., Chikurel, H., Dillon, P., Gaus, I., Guttman, J., Kraitzer, T., Kremer, S., Masciopinto, C., Pavelic, P., Picot-Colbeaux, G., Pettenati, M., Miotlinski, K., 2012. Use of groundwater models for prediction and optimisation of the behaviour of MAR sites. *Water Reclamation Technologies for Safe Managed Aquifer Recharge*, pp. 311–349.
- Laws, B.V., Dickenson, E.R.V., Johnson, T.A., Snyder, S.A., Drewes, J.E., 2011. Attenuation of contaminants of emerging concern during surface-spreading aquifer recharge. *Sci. Total Environ.* 409, 1087–1094. <https://doi.org/10.1016/j.scitotenv.2010.11.021>.
- Li, Zhang, Ma, Liu, Song, Li, 2018. An evaluation on the intra-day dynamics, seasonal variations and removal of selected pharmaceuticals and personal care products from urban wastewater treatment plants. *Sci. Total Environ.* 640–641, 1139–1147. <https://doi.org/10.1016/j.scitotenv.2018.05.362>.
- Liu, Y.-S., Ying, G.-G., Shareef, A., Kookana, R.S., 2011. Biodegradation of three selected benzotriazoles under aerobic and anaerobic conditions. *Water Res.* 45, 5005–5014. <https://doi.org/10.1016/j.watres.2011.07.001>.
- Liu, Y.-S., Ying, G.-G., Shareef, A., Kookana, R.S., 2013. Biodegradation of three selected benzotriazoles in aquifer materials under aerobic and anaerobic conditions. *J. Contam. Hydrol.* 151, 131–139. <https://doi.org/10.1016/j.jconhyd.2013.05.006>.
- Löffler, D., Römbke, J., Meller, M., Ternes, T.A., 2005. Environmental fate of pharmaceuticals in water/sediment systems. *Environ. Sci. Technol.* 39, 5209–5218. <https://doi.org/10.1021/es0484146>.
- Maeng, S.K., Sharma, S.K., Lekkerkerker-Teunissen, K., Amy, G.L., 2011. Occurrence and fate of bulk organic matter and pharmaceutically active compounds in managed aquifer recharge: a review. *Water Res.* 45, 3015–3033. <https://doi.org/10.1016/j.watres.2011.02.017>.
- Massmann, G., Sültenfuß, J., Dünnbier, U., Knappe, A., Taute, T., Pekdeger, A., 2008. Investigation of groundwater residence times during bank filtration in Berlin: a multi-tracer approach. *Hydrol. Process.* 22, 788–801. <https://doi.org/10.1002/hyp.6649>.
- Muntau, M., Schulz, M., Jewell, K.S., Hermes, N., Hübner, U., Ternes, T., Drewes, J.E., 2017. Evaluation of the short-term fate and transport of chemicals of emerging concern during soil-aquifer treatment using select transformation products as intrinsic redox-sensitive tracers. *Sci. Total Environ.* 583, 10–18. <https://doi.org/10.1016/j.scitotenv.2016.12.165>.
- Négre, P., Guerrot, C., Millot, R., 2007. Chemical and strontium isotope characterization of rainwater in France: influence of sources and hydrogeochemical implications. *Isot. Environ. Health Stud.* 43, 179–196. <https://doi.org/10.1080/10256010701550773>.
- Nham, H.T.T., Greskowiak, J., Nödler, K., Rahman, M.A., Spachos, T., Rusterberg, B., Massmann, G., Sauter, M., Licha, T., 2015. Modeling the transport behavior of 16 emerging organic contaminants during soil aquifer treatment. *Sci. Total Environ.* 514, 450–458. <https://doi.org/10.1016/j.scitotenv.2015.01.096>.
- Parker, J., Van Genuchten, M., 1984. Determining transport parameters from laboratory and field tracer experiments. *Va Agric. Exp. Sin. Bull.* 84–3, 1–47.
- Parkhurst, D.L., Appelo, C.A.J., 2013. Description of Input And Examples for PHREEQC Version 3: A Computer Program for Speciation, Batch-reaction, One-dimensional Transport, And Inverse Geochemical Calculations (Report No. 6-A43), Techniques And Methods. <https://doi.org/10.3133/tm6A43> Reston, VA.
- Patterson, B.M., Shackleton, M., Furness, A.J., Pearce, J., Descourvieres, C., Linge, K.L., Busetti, F., Spadek, T., 2010. Fate of nine recycled water trace organic contaminants and metal(loid)s during managed aquifer recharge into an anaerobic aquifer: column studies. *Water Res.* 44, 1471–1481. <https://doi.org/10.1016/j.watres.2009.10.044>.

- Patterson, B.M., Shackleton, M., Furness, A.J., Bekele, E., Pearce, J., Linge, K.L., Buseti, F., Spadek, T., Toze, S., 2011. Behaviour and fate of nine recycled water trace organics during managed aquifer recharge in an aerobic aquifer. *J. Contam. Hydrol.* 122, 53–62. <https://doi.org/10.1016/j.jconhyd.2010.11.003>.
- Pettenati, M., Picot-Colbeaux, G., Mathurin, F., Soulier, C., Togola, A., Devau, N., Lartigaut, C., Thomas, L., Aurouet, A., Thierion, C., Wissocq, A., Baïssat, M., Neyens, D., 2019. Novel monitoring- modelling systems to manage qualitative and quantitative status of coastal aquifers (Deliverable H2020-WATER No. D2.3.1). Demonstrating Synergies in Combined Natural And Engineered Processes for Wastertreatment Systems. AquaNES.
- Picot-Colbeaux, G., Devau, N., Pettenati, M., Akrou, R., Blanc, P., Thiéry, D., 2018. D3.2 Developments of a multi-scale modeling tool to describe the fate and transport of CECs, TPs and pathogens through IPR strategies (No. WaterJPI2013- FRAME Report). Challenges for a Challenging World – Joint Programming Initiative.
- Picot-Colbeaux, G., Mathurin, F., Pettenati, M., Nakache, F., Guillemoto, Q., Baïssat, M., Devau, N., Gosselin, M., Allain, D., Neyens, D., Lartigaut, C., Dufour, E., Togola, A., Depraz, O., Nauleau, F., 2021. Sustainable managed aquifer recharge (MAR) – soil aquifer treatment system to protect coastal ecosystem in Agon-Coutainville (Normandy), France. In: Zheng, Y., Ross, A., Villholth, K., Dillon, P. (Eds.), *Exemplary Case Studies of Sustainable And Economic Managed Aquifer Recharge*. UNESCO-IAH-GRIPP Publication. A UNESCO-IAH-GRIPP Publication.
- PubChem database, e. <https://pubchem.ncbi.nlm.nih.gov>. (Accessed 9 October 2021).
- Refsgaard, J.C., Henriksen, H.J., 2004. Modelling guidelines—terminology and guiding principles. *Adv. Water Resour.* 27, 71–82. <https://doi.org/10.1016/j.advwatres.2003.08.006>.
- Regnery, J., Wing, A.D., Alidina, M., Drewes, J.E., 2015. Biotransformation of trace organic chemicals during groundwater recharge: how useful are first-order rate constants? *J. Contam. Hydrol.* 179, 65–75. <https://doi.org/10.1016/j.jconhyd.2015.05.008>.
- Sabljčić, A., Güsten, H., Verhaar, H., Hermens, J., 1995. QSAR modelling of soil sorption. Improvements and systematics of log KOC vs. log KOW correlations. *Chemosphere* 31, 4489–4514. [https://doi.org/10.1016/0045-6535\(95\)00327-5](https://doi.org/10.1016/0045-6535(95)00327-5).
- Sanz-Prat, A., Greskowiak, J., Burke, V., Rivera Villarreyes, C.A., Krause, J., Monnikhoff, B., Sperlich, A., Schimmelpfennig, S., Duennbier, U., Massmann, G., 2020. A model-based analysis of the reactive transport behaviour of 37 trace organic compounds during field-scale bank filtration. *Water Res.* 173, 115523. <https://doi.org/10.1016/j.watres.2020.115523>.
- Schaffer, M., Boxberger, N., Börnick, H., Licha, T., Worch, E., 2012. Sorption influenced transport of ionizable pharmaceuticals onto a natural sandy aquifer sediment at different pH. *Chemosphere* 87, 513–520. <https://doi.org/10.1016/j.chemosphere.2011.12.053>.
- Schulze-Makuch, 2005. Longitudinal dispersivity data and implications for scaling behavior. *Groundwater* 43, 443–456. <https://doi.org/10.1111/j.1745-6584.2005.0051.x>.
- Sharma, L., Greskowiak, J., Ray, C., Eckert, P., Prommer, H., 2012. Elucidating temperature effects on seasonal variations of biogeochemical turnover rates during riverbank filtration. *J. Hydrol.* 428–429, 104–115. <https://doi.org/10.1016/j.jhydrol.2012.01.028>.
- Sprenger, C., Hartog, N., Hernández, M., Vilanova, E., Grützmacher, G., Scheibler, F., Hannappel, S., 2017. Inventory of managed aquifer recharge sites in Europe: historical development, current situation and perspectives. *Hydrogeol. J.* 25, 1909–1922. <https://doi.org/10.1007/s10040-017-1554-8>.
- Stein, K., Ramil, M., Fink, G., Sander, M., Ternes, T.A., 2008. Analysis and sorption of psychoactive drugs onto sediment. *Environ. Sci. Technol.* 42, 6415–6423. <https://doi.org/10.1021/es702959a>.
- Tang, G., Mayes, M.A., Parker, J.C., Jardine, P.M., 2010. CXTFIT/Excel—a modular adaptable code for parameter estimation, sensitivity analysis and uncertainty analysis for laboratory or field tracer experiments. *Comput. Geosci.* 36, 1200–1209. <https://doi.org/10.1016/j.cageo.2010.01.013>.
- Teijon, G., Candela, L., Tamoh, K., Molina-Díaz, A., Fernández-Alba, A.R., 2010. Occurrence of emerging contaminants, priority substances (2008/105/CE) and heavy metals in treated wastewater and groundwater at Depurbaix facility (Barcelona, Spain). *Sci. Total Environ.* 408, 3584–3595. <https://doi.org/10.1016/j.scitotenv.2010.04.041>.
- Ternes, T.A., 1998. Occurrence of drugs in German sewage treatment plants and rivers dedicated to professor Dr. Klaus Haberer on the occasion of his 70th birthday.1. *Water Res.* 32, 3245–3260. [https://doi.org/10.1016/S0043-1354\(98\)00099-2](https://doi.org/10.1016/S0043-1354(98)00099-2).
- Togola, A., Baran, N., Coureau, C., 2014. Advantages of online SPE coupled with UPLC/MS/MS for determining the fate of pesticides and pharmaceutical compounds. *Anal. Bioanal. Chem.* 406, 1181–1191. <https://doi.org/10.1007/s00216-013-7248-8>.
- Toride, N., Leij, F., Van Genuchten, M., 1995. 137. *Salin. Lab.*
- Tzoraki, O., Dokou, Z., Christodoulou, G., Gaganis, P., Karatzas, G., 2018. Assessing the efficiency of a coastal managed aquifer recharge (MAR) system in Cyprus. *Sci. Total Environ.* 626, 875–886. <https://doi.org/10.1016/j.scitotenv.2018.01.160>.
- Yamamoto, H., Nakamura, Yudai, Moriguchi, S., Nakamura, Yuki, Honda, Y., Tamura, I., Hirata, Y., Hayashi, A., Sekizawa, J., 2009. Persistence and partitioning of eight selected pharmaceuticals in the aquatic environment: laboratory photolysis, biodegradation, and sorption experiments. *Water Res.* 43, 351–362. <https://doi.org/10.1016/j.watres.2008.10.039>.